Molecular Phylogenetics and Evolution 83 (2015) 72–85

Contents lists available at ScienceDirect

Molecular Phylogenetics and Evolution

journal homepage: www.elsevier.com/locate/ympev

A dated molecular phylogeny of manta and devil rays (Mobulidae) based on mitogenome and nuclear sequences

Marloes Poortvliet [a,b,c,*], Jeanine L. Olsen [a], Donald A. Croll [b], Giacomo Bernardi [b], Kelly Newton [b], Spyros Kollias [c], John O'Sullivan [d], Daniel Fernando [e,f], Guy Stevens [f], Felipe Galván Magaña [g], Bernard Seret [h], Sabine Wintner [i,j], Galice Hoarau [c]

[a] Department of Marine Benthic Ecology and Evolution, Centre for Ecological and Evolutionary Studies, University of Groningen, Nijenborgh 7, 9747 AG Groningen, The Netherlands
[b] Department of Ecology & Evolutionary Biology, University of California Santa Cruz, 100 Shaffer Road, Santa Cruz, CA 95060, USA
[c] Faculty of Biosciences and Aquaculture, Universitetet i Nordland, Universitetsalleen 11, 8049 Bodø, Norway
[d] Monterey Bay Aquarium, 886 Cannery Row, Monterey, CA 93940, USA
[e] Department of Biology and Environmental Science, Linnaeus University, SE 39182 Kalmar, Sweden
[f] The Manta Trust, Catemwood House, Corscombe, Dorchester, Dorset DT2 0NT, United Kingdom
[g] Centro Interdisciplinario de Ciencias Marinas, Instituto Politécnico Nacional, Av. IPN s/n, La Paz, Baja California Sur 23096, Mexico
[h] Muséum national d'Histoire naturelle, Département Systématique et Evolution, CP 51, rue Buffon, 75231 Paris cedex 05, France
[i] KwaZulu-Natal Sharks Board, 1A Herrwood Drive, Umhlanga Rocks 4320, South Africa
[j] Biomedical Resource Unit, University of KwaZulu-Natal, Westville Campus, University Road, Westville 3600, South Africa

ARTICLE INFO

Article history:
Received 29 June 2014
Revised 7 September 2014
Accepted 8 October 2014
Available online 13 November 2014

Keywords:
Mitogenome
Phylogenetics
Molecular clock
Divergence times
Manta
Mobula

ABSTRACT

Manta and devil rays are an iconic group of globally distributed pelagic filter feeders, yet their evolutionary history remains enigmatic. We employed next generation sequencing of mitogenomes for nine of the 11 recognized species and two outgroups; as well as additional Sanger sequencing of two mitochondrial and two nuclear genes in an extended taxon sampling set. Analysis of the mitogenome coding regions in a Maximum Likelihood and Bayesian framework provided a well-resolved phylogeny. The deepest divergences distinguished three clades with high support, one containing *Manta birostris*, *Manta alfredi*, *Mobula tarapacana*, *Mobula japanica* and *Mobula mobular*; one containing *Mobula kuhlii*, *Mobula eregoodootenkee* and *Mobula thurstoni*; and one containing *Mobula munkiana*, *Mobula hypostoma* and *Mobula rochebrunei*. *Mobula* remains paraphyletic with the inclusion of *Manta*, a result that is in agreement with previous studies based on molecular and morphological data. A fossil-calibrated Bayesian random local clock analysis suggests that mobulids diverged from *Rhinoptera* around 30 Mya. Subsequent divergences are characterized by long internodes followed by short bursts of speciation extending from an initial episode of divergence in the Early and Middle Miocene (19–17 Mya) to a second episode during the Pliocene and Pleistocene (3.6 Mya – recent). Estimates of divergence dates overlap significantly with periods of global warming, during which upwelling intensity – and related high primary productivity in upwelling regions – decreased markedly. These periods are hypothesized to have led to fragmentation and isolation of feeding regions leading to possible regional extinctions, as well as the promotion of allopatric speciation. The closely shared evolutionary history of mobulids in combination with ongoing threats from fisheries and climate change effects on upwelling and food supply, reinforces the case for greater protection of this charismatic family of pelagic filter feeders.

1. Introduction

Manta and devil rays (Superorder: Batoidae, Order: Myliobatiformes, Family: Mobulidae[1]) represent one of the most

* Corresponding author at: Department of Marine Benthic Ecology and Evolution, Centre for Ecological and Evolutionary Studies, University of Groningen, Nijenborgh 7, 9747 AG Groningen, The Netherlands.
E-mail addresses: m.poortvliet@rug.nl (M. Poortvliet), J.L.Olsen@rug.nl (J.L. Olsen), dcroll@ucsc.edu (D.A. Croll), bernardi@ucsc.edu (G. Bernardi), newton@ucsc.edu (K. Newton), Spyros.Kollias@uin.no (S. Kollias), JOSullivan@mbayaq.org (J. O'Sullivan), daniel@mantatrust.org (D. Fernando), guy@mantatrust.org (G. Stevens), galvan.felipe@gmail.com (F. Galván Magaña), seret@mnhn.fr (B. Seret), wintner@shark.co.za (S. Wintner), Galice.Guillaume.Hoarau@uin.no (G. Hoarau).

http://dx.doi.org/10.1016/j.ympev.2014.10.012
1055-7903/

[1] Mobulids are alternatively considered as a subfamily (Mobulinae) of the family Myliobatidae (Bonaparte, 1838). We use Mobulidae, as it is the most widely used synonym in the literature (e.g., Gadig and Neto, 2014).

distinct groups of cartilaginous fishes. They display a dorso-ventrally flattened body with broad, well-developed pectoral fins and a whip-like tail. They are the largest (in disc width) extant group of rays inhabiting tropical, subtropical and warm temperate waters worldwide (Compagno and Last, 1999; Last and Stevens, 2009). Collectively referred to as mobulids, the two recognized genera (*Mobula*, Rafinesque-Schmaltz, 1810, and *Manta*, Bancroft, 1829) comprise 11 species. All are planktivores characterized by loss of dental function related to feeding (Adnet et al., 2012), the presence of cephalic lobes that direct prey into the mouth, and by a set of prebranchial filter plates (Bigelow and Schroeder, 1953; Coles, 1916; Cortés et al., 2008). Mobulids display life history traits that make them vulnerable to overexploitation (Dulvy et al., 2008, 2014; Garcia et al., 2008), i.e. matrotrophic reproduction (nourishment of embryos derived from the mother), large size at birth, slow growth, high maximum age (>30 years in *M. alfredi*, >20 years in *M. birostris* and >14 years in *M. japanica*), delayed age of first reproduction (3–10 years in *M. alfredi* and possibly 5–6 years in *M. japanica*) and low fecundity (one pup born every 1–3 years) (reviewed by Couturier et al., 2012; Cuevas-Zimbrón et al., 2012).

Despite their iconic status, the taxonomic history of mobulids is cluttered with competing hypotheses and little resolution. Most notably, and despite the formal separation into *Manta* and *Mobula*, it has been suggested that *Manta* is nested within the genus *Mobula* (reviewed by Aschliman, 2014). This is based on the analysis of three out of 11 mobulids with the mitochondrial genes NADH2 and NADH4, and the nuclear genes RAG1 and SCFD2 (Aschliman et al., 2012a), and an analysis of six out of 11 mobulids with the mitochondrial gene NADH2 (Naylor et al., 2012a); morphology (Adnet et al., 2012; Aschliman et al., 2012b; Gonzalez-Isais and Dominguez, 2004; Herman et al., 2000); and parasite evolution (Benz and Deets, 1988; Olson et al., 2010). Additionally, for several species it is still not clear whether they comprise distinct lineages or merely represent geographically separated morphological variants of the same species (Marshall and Bennett, 2010; Notarbartolo di Sciara, 1987). *Manta* is currently comprised of two species, the oceanic manta, *M. birostris* (Walbaum, 1792) and the reef manta *M. alfredi* (Krefft, 1868), and a tentatively identified but as of yet unclassified third species, present in the Atlantic (Marshall et al., 2009). *Mobula* contains nine currently recognized species: *M. japanica* (Müller and Henle, 1841), *M. mobular* (Bonnaterre, 1788), *M. tarapacana* (Philippi, 1892), *M. thurstoni* (Lloyd, 1908), *M. kuhlii* (Müller and Henle, 1841), *M. eregoodootenkee* (Bleeker, 1859), *M. hypostoma* (Bancroft, 1831), *M. rochebrunei* (Vaillant, 1879); and *M. munkiana* (Notarbartolo di Sciara, 1987). Morphologically, *Manta* is distinct from *Mobula* in exhibiting a terminal mouth, a broader head relative to maximum disc width (DW), and morphometrics of the spiracles (Compagno and Last, 1999; Notarbartolo di Sciara, 1987) and structure of filter plates (Paig-Tran et al., 2013). The two *Manta* species show differences in maximum DW (*M. birostris* and *M. alfredi*, 700 and 500 cm respectively), coloration patterns, dentition, denticle and spine morphology (Marshall et al., 2009). *Mobula* species share a ventral placement of the mouth, and can be distinguished from each other by maximum DW, coloration, skin, presence or absence of a vestigial caudal spine, structure of filter plates (Paig-Tran et al., 2013), and morphometrics of pectoral fins, tails, cephalic lobes and spiracles (Notarbartolo di Sciara, 1987). *M. birostris*, *M. alfredi*, *M. mobular*, *M. japanica* and *M. tarapacana* are among the larger rays in the family, with maximum DWs of 700, 500, 520, 370 and 310 cm respectively (Couturier et al., 2012). *M. thurstoni* has an intermediate maximum DW of 180 cm, and the remaining *Mobula* species are smaller, with a maximum DW of up to 130 cm (Couturier et al., 2012).

Geographical distribution of mobulids is, in general, correlated with maximum DW. Most species that attain large to intermediate maximum sizes have circumglobal or very wide distributions, with most species reported from the Pacific, Atlantic and Indian Oceans (Fig. 1A–E). Smaller species (e.g. *M. munkiana*, *M. hypostoma*, *M. rochebrunei*, *M. kuhlii* and *M. eregoodootenkee*) all have restricted geographical distributions, with *M. munkiana* recorded from the Eastern Pacific, *M. hypostoma* and *M. rochebrunei* recorded from the Western and Eastern Atlantic respectively, and *M. kuhlii* and *M. eregoodootenkee* both recorded from the Indo-West Pacific (IWP) (Fig. 1F–H). The only exception to this correlation is *M. mobular*, which attains a maximum DW comparable to that of *M. alfredi* (Pellegrin, 1901), but has a geographical range restricted to the Mediterranean Sea (Fig. 1A). However, *M. mobular* is morphologically highly similar to *M. japanica*, and although differences in tooth morphology suggest that *M. japanica* and *M. mobular* are separate species (Adnet et al., 2012), more detailed studies of morphology and genetics have yet to confirm whether *M. japanica* merits recognition.

Fossil, morphological and molecular data support the hypothesis that mobulids are one of the most derived groups of elasmobranchs and closely related to rhinopterids (cownose rays, genus *Rhinoptera*) within a polyphyletic clade of Myliobatidae (Naylor et al., 2012a; Aschliman et al., 2012a; Claeson et al., 2010; De Carvalho et al., 2004; Dunn et al., 2003; Lovejoy, 1996; McEachran and Aschliman, 2004; McEachran et al., 1996; Nishida, 1990; Shirai, 1996). However, a sister–clade relationship to a myliobatid–rhinopterid clade has also been proposed (Gonzalez-Isais and Dominguez, 2004) solely based on morphological data. Fossil remains show mobulid lineages with tooth morphology intermediate between durophageous (shell-crushing) and non-durophageous mobulids dating back to the Late Paleocene to Early Eocene (58.7–47.8 Mya) (Adnet et al., 2012). Modern mobulids do not occur in the fossil record until the Early Oligocene (~34 Mya) based on the first occurrence of teeth without strain-marks caused by biomechanical stress due to grinding-type feeding (Adnet et al., 2012). Fossils of extant species are much more recent, and date back only to the Late Miocene–Early Pliocene (11.61–3.6 Mya), except one tooth recovered possibly representative of *Manta* sp., which was tentatively dated as Early Oligocene (33.9–28.1 Mya). Recent records are limited to fossil teeth of *M. hypostoma* and *Manta* from the Late Miocene–Early Pliocene (Costa Rica, 11.61–3.6 Mya) (Laurito Mora, 1999), and of *Manta* from the Early Pliocene (Yorktown, USA, 5.332–3.6 Mya) (Bourdon, 1999), although the latter was classified as reminiscent of *M. japanica* and *M. mobular* by Adnet et al. (2012). Fossil teeth have also been recovered reminiscent of *M. japanica* and *M. mobular* from the Late Miocene–Early Pliocene (Costa Rica, 11.608–3.6 Mya) (Adnet et al., 2012; Laurito Mora, 1999). No fossil teeth have been attributed to *M. alfredi* due to its previously uncertain taxonomic status, but based on molecular data and the appearance of the first fossil *Manta* around 4.8 Mya (Bourdon, 1999; Cappetta and Stringer, 1970; Purdy et al., 2001; but see Adnet et al., 2012) it is thought that *M. alfredi* and *M. birostris* diverged within the last 1 My (Kashiwagi et al., 2012).

Phylogenetic analysis of mitochondrial DNA (mtDNA) is a widely used tool for delineating species relationships (Moritz, 1994) because of its fast rate of sequence evolution and rapid lineage sorting relative to the nuclear genome (Avise, 1989; Brown et al., 1982; Moore, 1995). However, mtDNA can be uninformative if only small portions of the mitogenome are used (Galtier et al., 2009). This is especially the case in lineages that display slow rates of mutation (Hoelzel et al., 2002; Morin et al., 2010), such as elasmobranchs and cetaceans (Martin et al., 1992; Martin and Palumbi, 1993; Nabholz et al., 2008), or when radiations occurred closely spaced in time (Vilstrup et al., 2011; Wielstra and Arntzen, 2011; Yu et al., 2007). Greater resolution can be achieved by increasing the amount of sequence data (Cummings et al., 1995; Morin

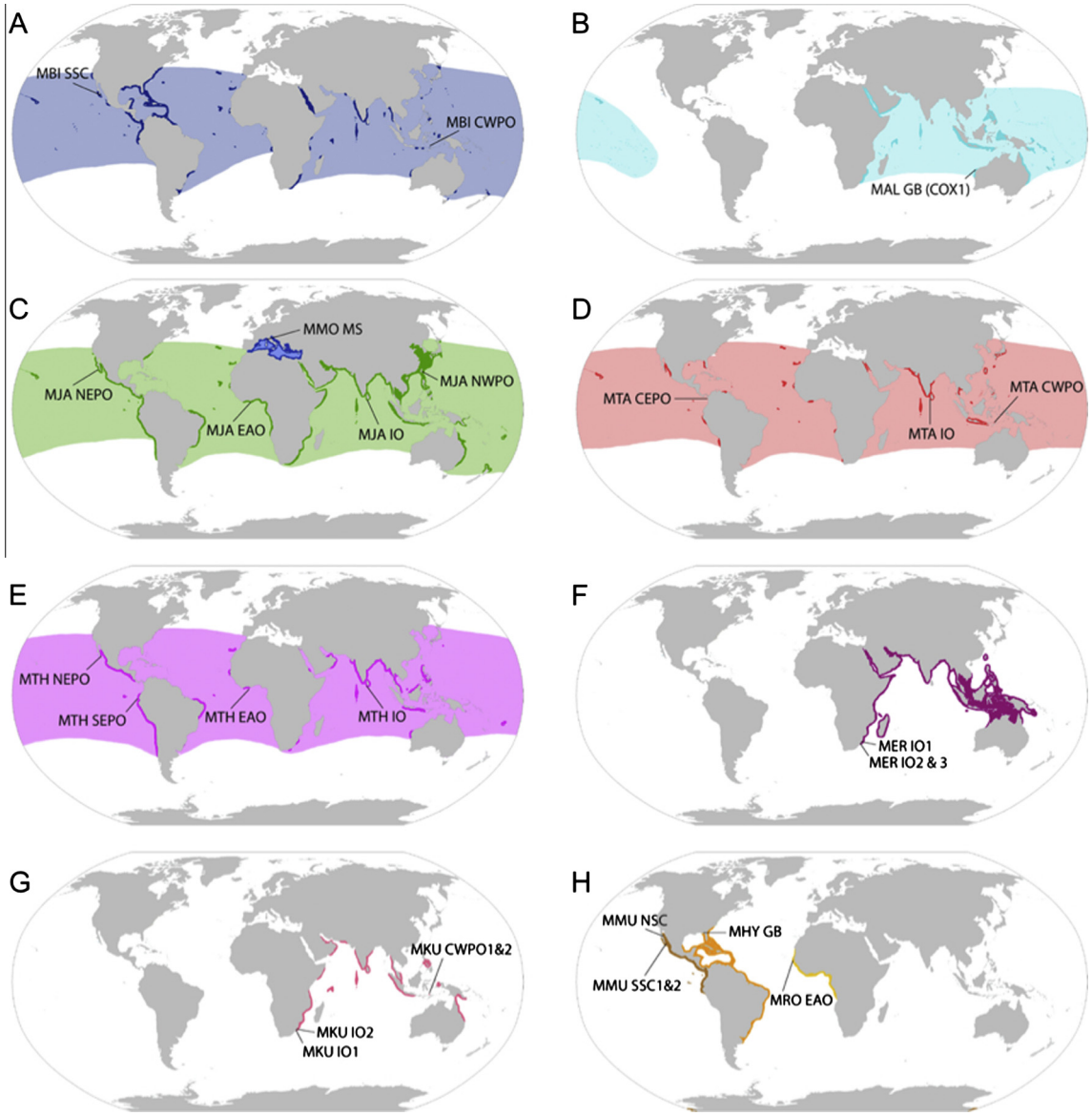

Fig. 1. Geographic distributions of all *Mobula* and *Manta* species. Maps A–E show confirmed locations (darker colors) and presumed range (lighter colors). A: *M. birostris*; B: *M. alfredi*; C: *M. japanica* (light and dark green) and *M. mobular* (light and dark blue); D: *M. tarapacana*; E: *M. thurstoni*; F: *M. eregoodootenkee*; G: *M. kuhlii*; H: *M. munkiana* (brown), *M. hypostoma* (orange) and *M. rochebrunei* (yellow). Sample abbreviations in Table 1. Maps have been reproduced with approval of the Manta Trust (www.mantatrust.org).

et al., 2010; Vilstrup et al., 2011; Wielstra and Arntzen, 2011; Yu et al., 2007), here the entire mitogenome. The advent of next-generation sequencing (NGS) now makes it easier and cheaper to rapidly and efficiently obtain large mitogenome data sets, in comparison with traditional Sanger sequencing.

In the present study, we: (1) use NGS of entire mitochondrial genomes, conventional Sanger sequencing of two nuclear and two mitochondrial genes to expand the taxon sampling, and supplementary GenBank sequences to reconstruct evolutionary relationships among all currently described mobulid species; (2) estimate divergence times between species based on two fossil dating points, the mitogenome tree and a random local molecular clock; (3) discuss the role of paleoclimatic changes in the evolutionary diversification and global biogeographic distribution of mobulids; and (4) discuss concerns and solutions for conservation of this group of cartilaginous fishes.

2. Methods

2.1. Sample collection and DNA extraction

Tissue samples were collected from all Mobulidae species (Table 1) except *M. alfredi*, for which GenBank sequences were used. Where possible, multiple samples per species were collected from widely spaced geographic locations. Samples from *M. hypostoma* (voucher no. MNHN-IC-1911-0207) and *M. rochebrunei* (voucher no. MNHN-IC-A-9967) were obtained from the Muséum national d'Histoire naturelle (Paris, France). A sample from *M. mobular* was obtained from the Museo di Storia Naturale di Firenze (Florence, Italy). Outgroup taxa, *Rhinoptera steindachneri* and *Myliobatis californica* ($n = 1$ and $n = 1$) (Dunn et al., 2003), were sampled from Sri Lanka and Mexico respectively (Table 1). Samples were preserved in 90% ethanol, in silica gel, freeze-dried, or

Table 1
Sample information. IUCN Red list codes: Least Concern (LC), Vulnerable (VU), Near Threatened (NT), Endangered (EN) and Data Deficient (DD). Location codes refer to the Southern Sea of Cortez (SSC), Northern Sea of Cortez (NSC), Central West Pacific Ocean (CWPO), Northeast Pacific Ocean (NEPO), Central East Pacific Ocean (CEPO), Southeast Pacific Ocean (SEPO), Northwest Pacific Ocean (NWPO), Central West Pacific Ocean (CWPO), Indian Ocean (IO), East Atlantic Ocean (EAO), Mediterranean Sea (MS) and GenBank sequences (GB). Also see Supplementary Table 1S.

Species	Species code	IUCN red list status	Location	Region	Latitude	Longitude	Collector, month, year
Manta birostris	MBI	VU	La Paz, Mexico	SSC	24°25′50N	110°20′21W	Galvan, June, 2000
M. birostris	MBI	VU	Ende, Indonesia	CWPO	8°51′15S	121°39′15E	Poortvliet, February, 2009
M. alfredi	MAL	VU	GenBank # JQ765532: West Australia. FJ235625 and FJ235624 see Kashiwagi et al. (2012)	GB	GenBank # JQ765532: 22°40′22S. FJ235625 and FJ235624 see Kashiwagi et al. (2012)	GenBank # JQ765532: 113°29′23E. FJ235625 and FJ235624 see Kashiwagi et al. (2012)	JQ765532: Cerutti-Pereyra et al. (2012). FJ235625 and FJ235624: Kashiwagi et al. (2012)
Mobula mobular	MMO	EN	Northern Tyrrhenian Sea, Italy	MS	43°19′54N	10°04′47E	Notarbartolo di Sciara & Serena, June, 1986
M. japanica	MJA	NT	P. A. Lopez Mateos, Mexico	NEPO	25°17′08N	111°55′59W	Poortvliet, July, 2008
M. japanica	MJA	NT	East Taiwan	NWPO	East Taiwan	East Taiwan	Unknown, April, 2002
M. japanica	MJA	NT	Negombo, Sri Lanka	IO	7°12′34N	79°50′03E	Fernando, May, 2011
M. japanica	MJA	NT	Lomé	EAO	6°5′37N	1°15′19E	Seret, March–July, 2011
M. tarapacana	MTA	DD	Nuqui, Colombia	CEPO	5°37′20N	77°42′00W	IATTC, January, 2011
M. tarapacana	MTA	DD	Lamakera, Indonesia	CWPO	8°26′07S	123°09′30E	Dewar, May, 2002
M. tarapacana	MTA	DD	Negombo, Sri Lanka	IO	7°12′34N	79°50′03E	Fernando, February, 2011
M. kuhlii	MKU	DD	Maumere, Indonesia	CWPO1	8°37′12S	122°13′12E	Poortvliet, March, 2009
M. kuhlii	MKU	DD	Maumere, Indonesia	CWPO2	8°37′12S	122°13′12E	Poortvliet, March, 2009
M. kuhlii	MKU	DD	Hibberdene, South Africa	IO1	30°35′20S	30°35′15E	KwaZulu-Natal Sharks Board, March, 2006
M. kuhlii	MKU	DD	Park Rynie, South Africa	IO2	30°19′07S	30°44′20E	KwaZulu-Natal Sharks Board, February, 2010
M. eregoodootenkee	MER	NT	Richards Bay, South Africa	IO1	28°51′08S	32°02′56E	KwaZulu-Natal Sharks Board, August, 2009
M. eregoodootenkee	MER	NT	Zinkwazi, South Africa	IO2	29°17′08S	31°26′14E	KwaZulu-Natal Sharks Board, September, 2004
M. eregoodootenkee	MER	NT	Zinkwazi, South Africa	IO3	29°17′08S	31°26′14E	KwaZulu-Natal Sharks Board, September, 2004
M. thurstoni	MTH	NT	La Paz, Mexico	NEPO	24°25′50N	110°20′21W	Croll, June, 2002
M. thurstoni	MTH	NT	Manta, Ecuador	SEPO	0°57′00S	80°42′58W	Galvan, May–September, 2010
M. thurstoni	MTH	NT	Negombo, Sri Lanka	IO	7°12′34N	79°50′03E	Fernando, June, 2011
M. hypostoma	MHY	DD	Gulf of Mexico	GB	29°48′28N	85°46′15W	Naylor et al. (2012b)
M. rochebrunei	MRO	VU	Senegal	EAO	15°00′0N	18°00′00W	MNHN (voucher no. MNHN-IC-A-9967)
M. munkiana	MMU	NT	La Paz, Mexico	SSC1	24°25′50N	110°20′21W	Croll, June, 2010
M. munkiana	MMU	NT	La Paz, Mexico	SSC2	24°25′50N	110°20′21W	Croll, June, 2010
M. munkiana	MMU	NT	Bahia de los Angeles, Mexico	NSC	29°07′12N	113°25′10W	Monterey Bay Aquarium, May, 2006
Myliobatis californica	–	LC	P. A. Lopez Mateos, Mexico	NEPO	25°17′08N	111°55′59W	Poortvliet, June, 2008
Rhinoptera steindachneri	–	NT	Negombo, Sri Lanka	IO	7°12′34N	79°50′03E	Fernando, September, 2011

air-dried (Table 1). Genomic DNA was extracted from muscle or tail tissue using Qiagen Blood and Tissue DNA purification kit (Qiagen, Valencia, CA, USA) following protocols suggested by the manufacturer; or according to a method developed by Hoarau et al. (2006) (Table 1S).

2.2. Mitogenome data set: High throughput sequencing and alignment

The entire mitogenome was sequenced for a total of 12 samples (Supplementary Table S1) following methods described by (Kollias et al., submitted for publication). Briefly, genomic DNA was sheared to fragments of ~260 bp (when necessary), using a Covaris S2 focused-ultrasonicator (Covaris, Woburn, USA). Library preparation (end repair, adaptor ligation, size selection) was conducted using an AB Library Builder™ System (Life Technologies, Carlsbad, USA) with an Ion Plus Library Kit for AB Library Builder™ System (Life Technologies, Carlsbad, USA), in combination with an Ion Xpress™ Barcode Adapters 1-16 Kit (Life Technologies, Carlsbad, USA). Libraries were amplified using an Ion Plus Library Kit for AB Library Builder™ System Protocol (Life Technologies, Carlsbad, USA), purified using an Agencourt® AMPure® XP Kit (Agencourt Biosciences, Beverly, USA), then pooled in equimolar amounts and concentrated using a PureLink® PCR Purification Kit (Life Technologies, Carlsbad, USA). The library pool was subsequently enriched using biotinylated single stranded DNA baits (MYbaits-1 system, www.mycroarray.com/mybaits/mybaits-custom.html) designed from the complete mitochondrial genome of *M. japanica* (NC_018784), and custom oligonucleotide blocking probes (Life Technologies, Carlsbad, USA and Thermo Fisher Scientific, Waltham, USA) designed to prevent the cross hybridization between Ion Torrent adapters during the hybridization step of the MYbaits protocol. Following enrichment, template preparation was conducted using an Ion PGM™ Template OT2 200 Kit (Life Technologies, Carlsbad, USA) and an Ion OneTouch™ 2 Instrument (Life Technologies, Carlsbad, USA). Sequencing was conducted using an Ion PGM™ 200 Sequencing Kit (Life Technologies, Carlsbad, USA) and an Ion 316™ Chip (Life Technologies, Carlsbad, USA) on an Ion Personal Genome Machine® (PGM™) System (Life Technologies, Carlsbad, USA). Protocols followed the manufacturer's instructions in all cases.

Mitogenome sequences of *M. japanica* were generated in a separate Ion PGM run, using PCR amplicons of *M. japanica* from

the Eastern Atlantic Ocean (EAO), North East Pacific Ocean (NEPO) and Indian Ocean (IO). First, the mitogenome (excluding the control region) was PCR amplified in overlapping amplicons of around 5 Kb with primers 72F in combination with 5023R, 3397F in combination with 9023R, 7915F in combination with 12875R and 11915F in combination with 15637R (Table 2S). Each PCR reaction contained 1.5 μl 10X Buffer, 0.3 μl KOD Hot Start DNA Polymerase (Toyoba, Osaka, Japan), 1 mM $MgSO_4$, 0.2 mM of each dNTP, 0.4 μM of forward and reverse primers and 10–100 ng of DNA. The cycling conditions consisted of 94 °C for 2 min, followed by 40 cycles of 20 s at 94 °C, 20 s at 52–54 °C (Supplementary Table 2S) and 3 min at 65 °C, with a final extension of 10 min at 65°C on a Geneamp v1.6 (Life Technologies, Carlsbad, USA). PCR products were gel-extracted using a Qiagen Gel Extraction kit (Qiagen, Valencia, USA), and 25 ng of each of four amplicons was pooled per sample. Library preparation (shearing, end repair, adaptor ligation, size selection) was conducted using an Ion Xpress™ Plus Fragment Library Kit (Life Technologies, Carlsbad, USA) with enzymatic shearing and an Ion Xpress™ Barcode Adapters 1-16 Kit (Life Technologies, Carlsbad, USA). Quantitation was conducted using an Ion Library Quantitation Kit (Life Technologies, Carlsbad, USA), after which equimolar amounts of each library were pooled. Emulsion PCR and enrichment were conducted using an Ion OneTouch™ 200 Template Kit (Life Technologies, Carlsbad, USA) on an Ion OneTouch™ Instrument (Life Technologies, Carlsbad, USA). Sequencing was conducted using an Ion PGM™ 200 Sequencing Kit (Life Technologies, Carlsbad, USA) and an Ion 316™ Chip (Life Technologies, Carlsbad, USA) on an Ion PGM™ System (Life Technologies, Carlsbad, USA). Protocols followed the manufacturers' instructions in all cases.

Sequence reads belonging to each barcoded library, from the two NGS runs, were mapped to the reference genome of *M. japanica* (NC_018784) using CLC Genomics Workbench v.6 (CLC bio, Aarhus, Denmark) with default mapping parameters. Of the 15 sequenced samples in the two runs, *M. hypostoma* (WAO) produced no barcoded reads, and therefore could not be included in the mitogenome data set. For the remaining 14 samples, consensus sequences were generated where coverage was >10 reads. Sections with lower coverage (5–9 reads) were inspected manually and included if all reads at a position were in agreement. Lower coverage areas were marked 'N'. The control region and flanking regions were excluded due to the presence of long tandem repeats (Poortvliet and Hoarau, 2013). All mitogenome consensus sequences have been deposited in GenBank (Supplementary Table 1S). Consensus sequences were aligned in CLC Genomics Workbench v.6 (CLC bio, Aarhus, Denmark). The alignment was checked manually, and homo-polymer stretches longer than four base pair were adjusted in length to fit the reading frame. Gaps in the alignment were coded as single events using the simple gap coding method of Simmons and Ochoterena (2000), implemented in the software SeqState 1.4.1. (Müller, 2005).

2.3. COX1/NADH5/RAG1/HEMO data set: PCR amplification, sequencing and sequence alignment

To allow for greater taxon sampling, 2–5 specimens of each species (when available) were PCR amplified and sequenced for two mitochondrial genes (cytochrome oxidase subunit 1, COX1; and NADH dehydrogenase subunit 5, NADH5) and two nuclear genes (recombination activating protein 1, RAG1; and Hemoglobin-alpha, HEMO). A 10-μl PCR reaction contained 0.1 μl HotMaster taq (5 PRIME, Hamburg, Germany), 1 μl PCR buffer (10X), 0.25 mM of each dNTP, 0.2 μM of each primer (Table 1S), and 10–100 ng of genomic DNA. Cycling conditions consisted of: 94 °C for 2 min, followed by 40 cycles of 94 °C for 20 s, 54–58 °C for 20 s (Supplementary Table 2S) and 65 °C for 60 s, with a final extension of 65 °C for 10 min. Cleaned PCR products (ExoSap, Amersham, Biosciences) were sequenced in both directions using 0.25 μM PCR primers, with BigDye Terminator v3.1 cycle sequencing kit (Applied Biosystems, Foster City, USA) following the recommended protocol. Sequences were visualized on an Applied Biosystems 3130xl automated sequencer (Applied Biosystems, Foster City, USA). All sequences have been deposited in GenBank (Supplementary Table 1S).

To allow for the phylogenetic placement of *M. alfredi*, for which we had no samples, COX1, NADH5 and RAG1 sequences available from GenBank (Accession no. JQ765532, FJ235625 and FJ235624 respectively) were included in the data set.

DNA from *M. mobular* (MS), *M. hypostoma* (WAO) and *M. rochebrunei* (EAO) was too degraded for PCR amplification. Instead, COX1, NADH2, RAG1 and HEMO were sequenced using biotinylated single stranded DNA baits and Ion PGM technology (Life Technologies, Carlsbad, USA), following methods described in Kollias et al. (submitted for publication) and as briefly outlined above. Baits were designed based on the mitogenome sequence available from GenBank (NC_018784), as well as RAG1 and HEMO sequences generated in this study. NGS of *M. hypostoma* was unsuccessful and no appropriate sequences were available from GenBank. Therefore we were unable to include this species in this dataset (but see NADH2 data set for phylogenetic analysis of *M. hypostoma*). NGS of nuclear sequences of *M. rochebrunei* was also unsuccessful. Therefore we were unable to include this species in this data set (but see mitogenome data set for phylogenetic analysis of *M. rochebrunei*).

Sequences were aligned and edited using the software Geneious 5.6 (BioMatters, Auckland, New Zealand). A separate alignment was created with only nuclear sequences (RAG1 and HEMO), which we refer to as the 'nuclear data set'. In cases where the RAG1 and HEMO genes were heterozygous (as inferred from double peaks in chromatograms) at single base positions, the International Union of Pure and Applied Chemistry (IUPAC) codes for the ambiguous nucleotide base calls were used. Gaps in both alignments were coded as single events using the simple gap coding method of Simmons and Ochoterena (2000), implemented in SeqState 1.4.1. (Müller, 2005).

2.4. NAHD2 data set: Sequence alignment

To allow for phylogenetic placement of *M. hypostoma*, a NADH subunit 2 (NADH2) sequence of *M. hypostoma* (GenBank JQ518837) was aligned with the NADH2 portion of the mitogenome data set using CLC Genomics Workbench v6 (CLC bio, Aarhus, Denmark). The alignment was checked manually, and homo-polymer stretches longer than four base pair were adjusted in length to fit the reading frame. Gaps in the alignment were coded as single events using the simple gap coding method of Simmons and Ochoterena (2000), implemented in SeqState 1.4.1 (Müller, 2005).

2.5. Model selection, phylogenetic analyses and confidence

The optimal partitioning scheme and models of nucleotide substitution for each data set were analyzed using PartitionFinder v1.1.1 (Lanfear et al., 2012), which provides an objective method for the assessment of these criteria, without the need for *a priori* groupings. The mitogenome alignment was separated into single codon positions and individual rRNAs and tRNAs; the COX1/NADH5/RAG1/HEMO alignment was separated into single codon positions, except the gene HEMO because, although sequences were straightforward to align, the reading frame could not be assessed reliably due to the presence of several long indels; the nuclear data set was separated into single codon positions; and finally, the NADH2 alignment was separated into single codon

positions. Optimal partitioning and nucleotide substitution models were subsequently analyzed using the Bayesian Information Criteria (BIC) for all data sets. Optimal partitioning and nucleotide substitution models are listed in Supplementary Table 3S.

For each data set (mitogenome, COX1/NADH5/RAG1/HEMO, nuclear and NADH2), Bayesian Inference (BI) topologies were generated using MrBayes v3.2.1 (Huelsenbeck and Ronquist, 2001) following the partitioning scheme and models of evolution suggested by PartitionFinder (Supplementary Table 3S) in two independent runs of 10 million generations with 3 chains (one cold, two heated) and sampling every 3000 generations. Where PartitionFinder selected a mixed distribution model of among-site rate variation (I + G), only a gamma distribution was implemented, as parameters estimated under the I + G model can be highly correlated, especially when only a small number of sequences are considered (Sullivan et al., 1999). Convergence of the two parallel runs was examined in Tracer v1.5 (Rambaut and Drummond, 2009), by confirming that ESS values were above 200, and by investigating whether the log-likelihood scores of the two parallel runs converged to similar values following the burn-in period. Posterior probabilities (PP) were estimated by sampling trees from the PP distribution. Post burn-in trees were summarized and a 50% majority rule consensus tree was built in MrBayes v.3.2.1. BI branches with PP values of <80 were collapsed using the software Archeaopteryx v0.9813 (Han and Zmasek, 2009). Maximum Likelihood (ML) topologies and 1000 bootstrap (BS) replicates were generated with RaxML v7.7.8 (Stamatakis, 2006), giving each partition suggested by PartitionFinder (Table 3S) its own GTR + CAT model of evolution in two independent analyses per alignment.

2.6. Divergence time estimation

Divergence times and substitution rates were estimated using the 13 gene regions of the mitogenome dataset and two fossil calibration points in the software BEAST v1.7.5 (Drummond et al., 2012).

Standard models of evolution implemented in BEAST assume mutual independence among sites. Because secondary structure of tRNA and rRNA regions of the mitogenome can violate this assumption (Dixon and Hillis, 1993), all RNA regions were removed from the mitogenome data set, leaving only the 13 gene regions (this data set is referred to as the 'mitogenome BEAST data set'). Each gene was separated into single codon positions and the optimal partitioning and evolutionary models were selected based on the BIC selection criteria in the software PartitionFinder v1.1.1 (Lanfear et al., 2012). The resulting optimal partitioning scheme and evolutionary models (Supplementary Table 3S) were used in all subsequent BEAST v1.7.5 analyses. Where PartitionFinder selected a mixed distribution model of among-site rate variation (I + G), only a gamma distribution was implemented (Sullivan et al., 1999). Where PartitionFinder selected a GTR model of evolution, a HKY model was implemented (see Table 3S), as a GTR model proved too parameter-rich for our data (Drummond et al., 2002).

Exploratory runs with either a lognormal relaxed clock (LNRC) or a random local clock (RLC) (Drummond and Suchard, 2010), both in combination with a birth–death (BD) prior for rates of cladogenesis (Drummond and Rambaut, 2007), were conducted. Both clock models resulted in substantial rate variation between different mobulid clades. Therefore, we chose to conduct further analyses using the random local clock (RLC) model in combination with a BD prior for rates of cladogenesis, as rate variation violates the assumptions of the LNRC model (Drummond and Suchard, 2010). Three runs were conducted of 50 million generations each, with sampling every 5000 generations. The software Tracer v1.5 (Rambaut and Drummond, 2009) was used to quantify effective sample sizes (ESS) for model parameters, and the 'compare' command in AWTY (Nylander et al., 2008) was used to assess convergence, with 10% of each run discarded as burn-in. Runs were combined using LogCombiner v1.7.5 (Drummond et al., 2012), and a time tree was obtained using TreeAnnotator v1.7.5 (Drummond et al., 2012).

Based on the oldest occurrence of true *Mobula* from the Late Oligocene (28.1–23.03 Mya) (Case, 1980; Cicimurri and Knight, 2009) we dated the divergence of basal mobulids to 28.1–23.03 Mya (Supplementary Table 4S). Fossils of *Manta* from the Late Miocene–Early Pliocene were used to date the split between *M. japanica*/*M. mobular* and *Manta* to 11.61–3.6 Mya (Laurito Mora, 1999) (Supplementary Table 4S). Priors with a normal distribution were used for both calibration points, with the minimum and maximum bounds for each calibration point (e.g. 28.1 and 23.03 respectively, and 11.61 and 3.6 My respectively) implemented with the 95% percentile of the distribution.

Although inadequate by themselves, fossil material from the Pliocene (5.33–3.6 Mya), which were classified as either *Manta* (Bourdon, 1999) or as reminiscent of *M. japanica*/*M. mobular* (Adnet et al., 2012), and fossils reminiscent of *M. japanica*/*M. mobular* from the Late Miocene-Early Pliocene (11.61–3.6 Mya) (Laurito Mora, 1999), were used in support of the two key dating points. A single tooth recovered from the Early Oligocene (33.9–28.1) reminiscent of *Manta* sp.(Picot et al., 2008), but which displays marked differences to the younger form (Adnet et al., 2012), was deemed too uncertain for use as a fossil calibration point for the divergence between *Manta* and *M. japanica*/*M. mobular*.

The species *M. hypostoma* and *M. alfredi* were not included in the mitogenome BEAST data set, due to lack of data and samples respectively. Therefore, we manually calculated divergence dates for these species assuming $d_A = 2\lambda T$, where d_A is the average number of net nucleotide substitutions per nucleotide site between species, λ is the substitution rate, and T is divergence time in years. Estimates of d_A between *M. hypostoma* and *M. rochebrunei* and between *M. birostris* and *M. alfredi* were calculated using the software MEGA v5.0 (Tamura et al., 2011) based on NADH2 sequences, and concatenated COX1 and NADH5 sequences for *M. hypostoma* and *M. alfredi* respectively, using the Tamura-Nei (Tamura et al., 2011) model as identified by jModelTest v0.1 (Posada, 2008). Estimates of λ of were obtained from our BEAST analyses (rates of *M. rochebrunei* and *M. birostris* for calculations of divergence dates of *M. hypostoma* and *M. alfredi* respectively).

3. Results

3.1. Phylogenetic inference and support

Mitogenome data set. NGS sequencing results (percent coverage, coverage depth range and coverage depth average) are reported in Supplementary Table 1S. The alignment consisted of 15387 nucleotides (nts) (11,470 nts protein coding DNA, 1350 nts rRNA and 1564 nts tRNA). The alignment contained a total of 89 indels, ranging from 1 to 9 nts in length. Pairwise sequence divergence among mobulid species ranged from 0.1% between *M. japanica* and *M. mobular*, to 14.8% between *M. munkiana* and *M. birostris*. The software PartitionFinder identified 11 partitions (Table 3S). The ML and BI trees (Fig. 2) were highly congruent and shared high support values: 8 out of 9 inter-specific nodes show both BI PP and ML BS values >99%. Mobulids formed three clades, one containing the two *Manta* species, *M. tarapacana*, *M. japanica* and *M. mobular*; one containing *M. kuhlii*, *M. eregoodootenkee* and *M. thurstoni*; and one containing *M. munkiana*, *M. hypostoma* and *M. rochebrunei*.

COX1/NADH5/RAG1/HEMO data set. The alignment consisted of 2285 nts: 502 nts for COX1, 669 nts for NADH5, 419 nts for RAG1 and 695 nts for HEMO. The final alignment contained a total

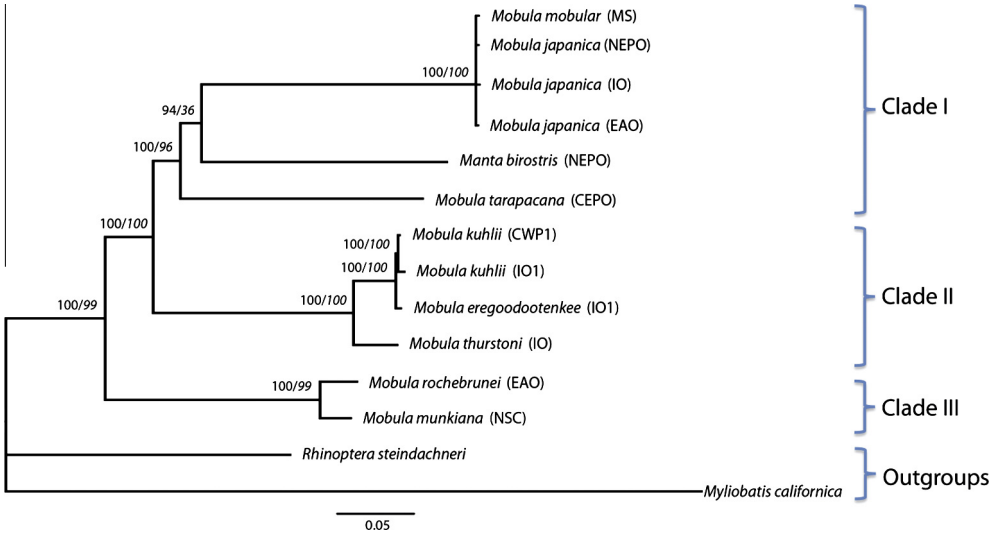

Fig. 2. Bayesian phylogeny based on the mitogenome data set. Support values above nodes (BI PP/*MLBS*). Nodes with BI PP values <80 are collapsed.

of 7 indels, ranging from 1 to 257 nts in length. Total pairwise sequence divergence ranged between 0–8.8%, 0–9.3%, 0–0.4% and 0–2.8%, for COX1, NADH5, RAG1 and HEMO respectively. The software PartitionFinder identified 5 partitions (Supplementary Table 3S). BI and ML trees (Fig. 3) produced the same three clades as the mitogenome data set and also with high support. Within clade resolution varied, with Clade I forming a polytomy. Within this polytomy, *M. alfredi* was sister species to *M. birostris* with high support (100/100). The data set containing only nuclear sequences (nuclear data set) is generally in agreement with results based on the *COX1/NADH5/RAG1/HEMO* data set. BI and ML analyses (Supplementary Fig. 1S) recovered Clade II with high support (100/100). All other species were contained in a polytomy.

NADH2 data set. The NADH2 data set consisted of 1044 nts and total sequence divergence ranged from 0% between *M. mobular* and *M. japanica* to 20% between *M. hypostoma* and *M. japanica*. The

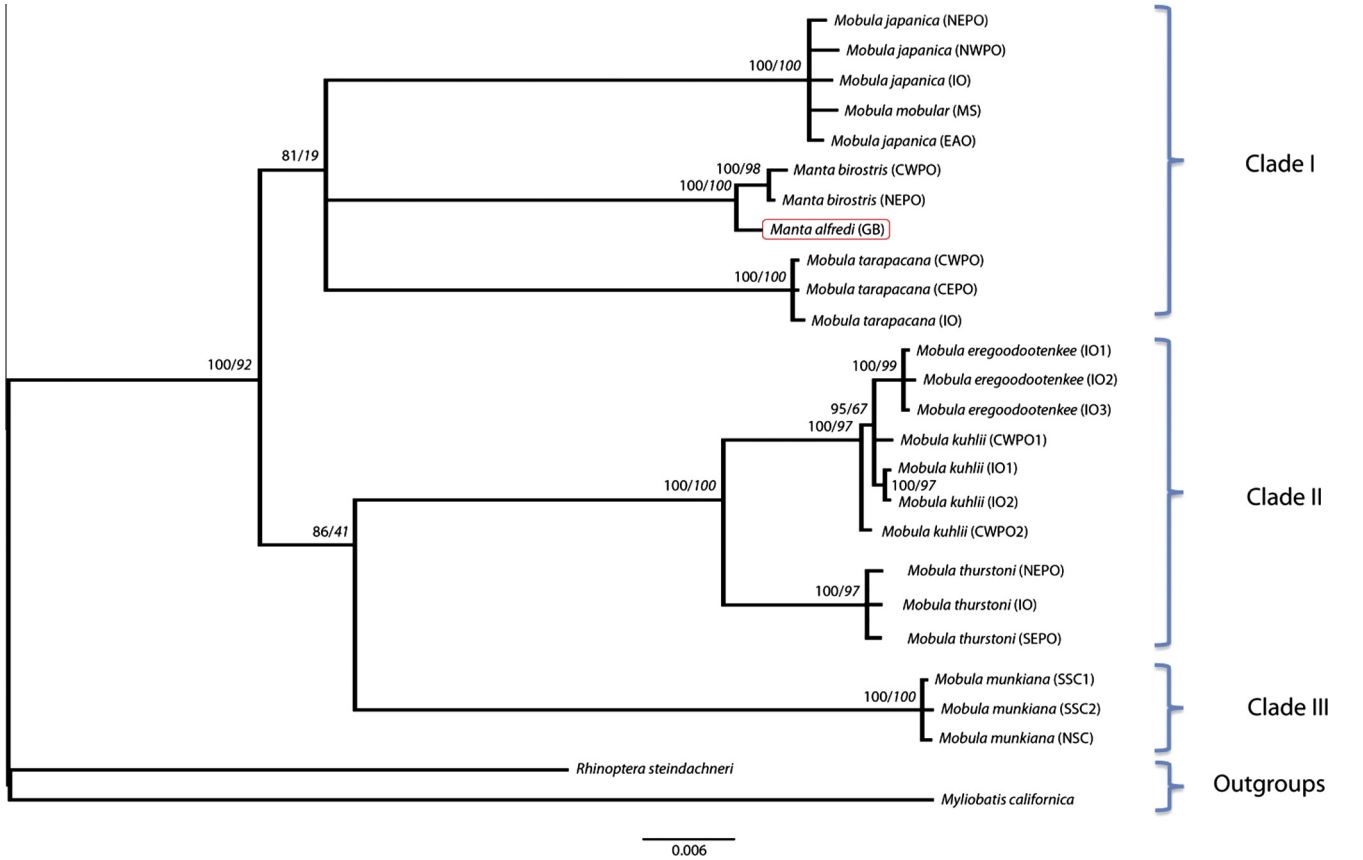

Fig. 3. Bayesian phylogeny based on the COX1/NADH5/HEMO/RAG1 data set. Support values above nodes (BI PP/ML *BS*). Nodes with BI PP values <80 are collapsed. The placement of *M. alfredi* as sister species to *M. birostris* is based on GenBank sequences of COX1, NADH5 and RAG1.

software PartitionFinder identified 3 partitions (Supplementary Table 3S). The NADH2 tree (Supplementary Fig. 2S) formed a polytomy, which included all mobulids and outgroup species. Within this polytomy, two out of the three clades found with the mitogenome and COX1/NADH5/RAG1/HEMO data sets are produced here (Clades II and III), also with high support (100/100). *M. hypostoma* falls in Clade III and as sister species to *M. rochebrunei* with high support (100/100).

3.2. Divergence time estimation

Tree topologies based on the three mitogenome BEAST runs were congruent, and in agreement with our mitogenome BI and ML analyses. The average estimated mean rate of nucleotide substitution in mobulids was 8.82×0^{-09} (95% HPD: $7.15 \times 10^{-09} - 10.77 \times 10^{-09}$). Rate estimates differed slightly among clades (Fig. 4 and Supplementary Table 5S), with the higher boundary of the 95% highest posterior density (HPD) of Clade I (combined 95% HPDs: $1.8 \times 10^{-09} - 12.8 \times 10^{-09}$) being almost twice as high as that of Clades II + III (combined 95% HPDs: $6.6 \times 10^{-09} - 9.8 \times 10^{-09}$).

Using the best fossil dating points for calibration, divergence between *M. californica* and *R. steinachneri* was dated at 48.81 Mya (node 1, Fig. 4), and divergence of the basal mobulids at 30.12 Mya (node 2, Fig. 4). Divergences between the three clades (nodes 3 and 4, Fig. 4) occurred between 22.27 and 19.59 Mya. Extant mobulids diverged during two periods: between 18.29 and 17.46 Mya (nodes 5 and 6, Fig. 4), and between 3.66 and 0.36 Mya (nodes 10, 11 and 13, Fig. 4). All rate and date estimates and 95% HPD intervals can be found in Supplementary Table 5S.

Based on d_A estimates and rate of nucleotide substitution of the most closely related lineages derived from the mitogenome BEAST data set, divergence between *M. rochebrunei* and *M. hypostoma* was estimated at 1.1 Mya, and divergence between *M. birostris* and *M. alfredi* at 0.03 Mya.

4. Discussion

4.1. The molecular clock, age estimates and the fossil record

It is well established that elasmobranchs exhibit nucleotide substitution rates that are slow relative to mammals (Martin et al., 1992). The reasons for this are less clear, although metabolic rate has been suggested as the most likely correlate for slow molecular rates in elasmobranchs (Martin, 1999). Estimates of the number of nucleotide substitutions per site per year ($S\ s^{-1}\ y^{-1}$) in elasmobranchs vary between 0.7×10^{-09} and 1.15×10^{-08} (reviewed by Dudgeon et al., 2012), which is approximately an order of magnitude slower than rates found in mammals. Our estimate of an average rate of $S\ s^{-1}\ y^{-1}$ in mobulids of 8.82×10^{-09} (95% HPD: $7.15 \times 10^{-09} - 10.77 \times 10^{-09}$) falls within the range estimated for elasmobranchs.

Shifts in nucleotide substitution rate both within and among lineages are a pervasive phenomenon across the Tree of Life (Britten, 1986; Martin and Palumbi, 1993; Wu and Li, 1985) including within the Carcharhiniformes and Lamniformes (Martin, 1995) and also within the Myliobatiformes (Dunn et al., 2003). Although no specific rates were given, Dunn et al. (2003) compared mitochondrial nucleotide substitution rates among species representing all of the myliobatoid families and found evidence for rate changes in *Torpedo*, *Raja*, *Gymnura*, *Urobatis*, *Potomatrygon*, *Rhinobatos* and *Rhinoptera* as compared to a null distribution. *M. birostris* was also included in that study but did not show a rate change as compared to the null distribution. However, within the Mobulidae we found evidence for a slight positive shift in

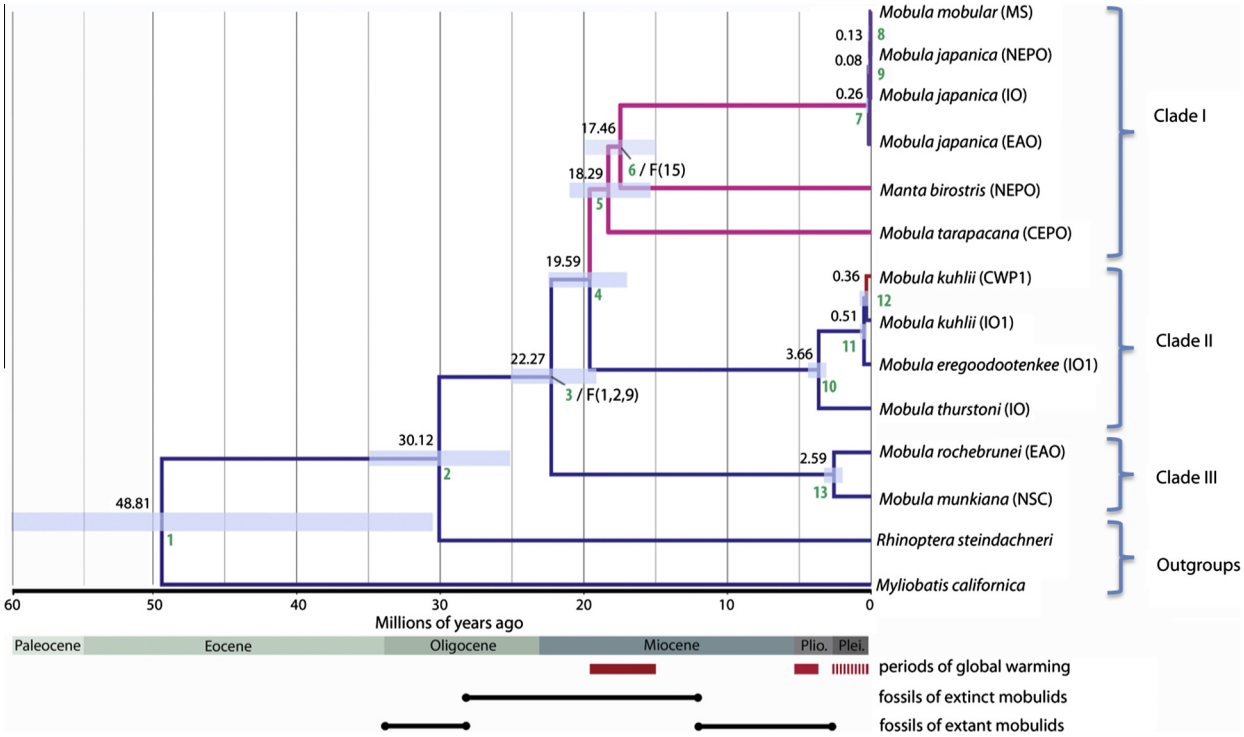

Fig. 4. Divergence time estimates based on analysis of the mitogenome BEAST data set. Point estimates of ages are given above each node and transparent blue horizontal bars denote age (95% highest posterior density). Branch colors show relative nucleotide substitution rates (blue is slow, purple intermediate, red fast. F(1, 2, 9) and F(15) denote fossil calibration points (numbers 1, 2, 9 and 15 refer to Supplementary Table S4). Green numbers on nodes are explained in the text. Red bars below the epoch bar denote periods of global warming and associated low upwelling intensities. Black lines below that denote timing of occurrence of extinct and extant mobulid species based on the fossil record (see Supplementary Table S4).

nucleotide substitution rate accompanying the divergence of Clade I, and an increase along the *M. kuhlii* lineage within Clade II.

There is currently no generalized explanation for the causes of increased or decreased nucleotide substitution rates. As estimates of branch length are dependent on sequence substitution models, model misspecifications can have a large influences on rate estimates (Kelchner and Thomas, 2007; Revell et al., 2005). Although the Bayesian approach implemented in BEAST does account for model uncertainty by varying model parameters during MCMC searches (Drummond and Rambaut, 2007), we cannot exclude that the infered shifts in substitution rate are the consequence of model misspecification. However, if small, fragmented and genetically isolated founder populations characterize most speciation events in mobulids, or if effective population sizes strongly fluctuated due to for example paleoclimatic variation, changes in effective population size (N_e) of incipient species or populations might have some bearing on the shifts in nucleotide substitution rates found in this study. Recent studies indicate that increases in substitution rates can be caused by a reduction in effective population size (Woolfit, 2009). In species with a smaller N_e, selection plays a less important role, causing slightly deleterious mutations to be fixed at an elevated rate. The same pattern is repeated across genomic regions with smaller N_e, such as regions with low recombination, in which linkage between weakly selected loci reduces the effectiveness of selection (Haddrill et al., 2007; Presgraves, 2005). Conversely, temporally increased substitution rates have also been found in lineages that had undergone population size expansions, due to the fixation of slightly advantageous back-mutations (Charlesworth and Eyre-Walker, 2007). Below, we discuss paleoclimatic variables that could have affected mobulid effective population sizes.

Based on our two fossil calibration points and the mitogenome-BEAST analysis, we date the divergence of *Myliobatis californica* and *Rhinoptera steindachneri* to ~48 Mya (node 1, fig. 4), which is in agreement with the occurrence of the first fossil rhinopterids between 56.0 and 33.9 Mya (Cappetta, 1987, 2006). Our estimate of subsequent divergence between *Rhinoptera* and the mobulid lineage (34.88–25.33 Mya, node 2, fig. 4) largely overlaps with an estimate by Aschliman et al. (2012a,b) (29.9–22.6 Mya) based on mitogenomes in combination with fossil calibration points external to the mobulid clade. However, their estimate was later suggested to be too recent (Aschliman, 2014), and to be more in line with estimates by Adnet et al. (2012). Adnet et al. (2012) estimated the divergence between these two lineages at around 50 Mya based on fossil teeth of the oldest putative mobulid *Burnhamia* (59.2–47.8 Mya), now extinct (Cappetta, 1985; Pfeil, 1981; Woodward, 1889), and on the first occurrence of fossil rhinopterids. *Burnhamia* is one of several extinct genera that have been compared or affiliated to mobulids based on their tooth morphologies; however, the taxonomic positions of these genera are still debated. Fossils of *Burnhamia*, which include three extinct species, were originally placed in the genus *Rhinoptera* (Woodward, 1889) but later attributed to a new genus among mobulids based on an apparent absence of biomechanical stress marks on the teeth, as seen in teeth of modern filter feeding mobulids (Cappetta, 1975). Our estimate for the divergence between *Rhinoptera* and the mobulid lineage suggests that *Burnhamia* should be placed outside of the mobulid lineage. However, as discussed earlier, we cannot exclude the possibility that our inferred timing for the rise of the mobulid lineage (~30 Mya) is the consequence of model misspecifications.

Within the extant mobulids, one of our estimates of divergence time is not congruent with the estimate based on the fossil record; fossil teeth of *M.* cf. *hypostoma* first occurred in the Middle Miocene and Pliocene (11.6–3.6 Mya) (Laurito Mora, 1999), much earlier than our estimate of ~1.1 Mya based on the formula $d_A = 2\lambda T$. Since we were unable to include mitogenome sequences of *M. hypostoma* in our BEAST analysis, it is possible that our divergence time estimate is too recent, and that the actual divergence of this species is much older. Alternatively, provided that our estimate is correct, tooth morphology of *M. hypostoma* (Adnet et al., 2012) could represent the ancestral state for (*M. hypostoma* + *M. rochebrunei*), with a reversal in the latter species.

4.2. Patterns of mobulid evolution

Divergences within the mobulid clade are characterized by long internodes extending from the base of each clade to its subsequent radiation starting around 3.6 Mya. This pattern is most notable in Clades II and III; however, a similar pattern is repeated in Clade I, where early radiations within the clade between 19 and 17 Mya are followed by long interior branches and the subsequent diversification of *Manta* less than 1 Mya. Punctuated patterns are common across the Tree of Life, including all major lineages of batoid rays (Aschliman et al., 2012a). Rapid radiations are often associated with key innovations, meta-community dynamics, environmental change and/or accelerated rates of molecular evolution (reviewed by Crisp and Cook, 2009). Alternatively, long interior branches can be the result of extinction events that prune internal branches while preserving older lineages; or even a combination of extinction alternated by bursts of divergence (Crisp and Cook, 2009). Discriminating among scenarios is difficult, especially when taxon sampling is limited. In that case, the fossil record, in combination with correlations between phylogenetic topologies and paleo-climatic events can provide clues about possible drivers of the observed pattern. For example, Aschliman et al. (2012a) attributed the pattern observed in the batoid ray phylogeny to an extinction event around the K/T boundary, owing to the higher survival rate of older lineages (families) relative to internal branches (genera).

Although fossil remains of mobulids are limited to isolated teeth, and are relatively scarce in marine deposits, five to eight extinct mobulid species are currently counted (reviewed by Adnet et al., 2012). These species are known from Oligocene and Miocene deposits (28.1–11.6 Mya), but had disappeared from the fossil record by 11 Mya. This suggests that the pattern of mobulid radiation is, at least partly, caused by an extinction event during this period. However, the occurrence of three stages of diversification at different rates (e.g. fast/slow/fast), a combination of factors (e.g. rate changes and extinctions), or model misspecifications cannot be excluded. Below, we discuss possible drivers and mechanisms of mobulid speciation.

4.3. Mechanisms and drivers of mobulid speciation

Early evolution of mobulids probably occurred during the Oligocene epoch (33.9–23.03 Mya), in the Atlantic and Tethyan Oceans based on locations of recovered fossils (reviewed by Adnet et al., 2012) (Fig. 5). The Oligocene was a period marked by large climatic changes, which profoundly affected conditions experienced by pelagic marine organisms. After the global warmth of the Paleocene and Early Eocene, the warm 'greenhouse' world of the early Eocene evolved into the glacial 'icehouse' conditions of the early Oligocene, with rapid onset of Antarctic glaciation around 34 Mya (Zachos et al., 2001). Cooling of the oceans, in conjunction with the opening of the Drake Passage around the tip of South America, produced regions where cold and nutrient-rich polar water mixed with warmer waters, increasing deep mixing and the intensity of zonal winds. These changes facilitated the upwelling of nutrient-rich deep water greatly boosting productivity in various locations, including in the Tropical and Subtropical Atlantic Ocean (Boersma and Silva, 1991; Suto et al., 2012; Zachos et al., 1996).

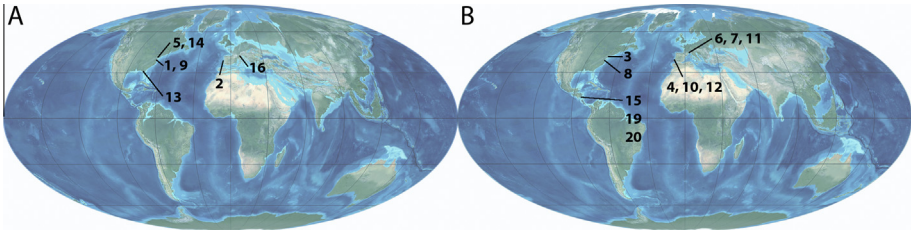

Fig. 5. Maps of continental arrangement during evolution of the mobulid lineage, with locations of fossil mobulid teeth. (A) Oligocene (33.9–23.03); (B) Miocene (23.03–5.33 Mya). Black numbers refer to Supplementary Table 4S. Maps have been reproduced with approval from the authors (Oligocene map: Blakey, 2008; Miocene map: http://jan.ucc.nau.edu/~rcb7/).

The timing of the development of the filter-feeding strategy in batoids – a key innovation within this clade-corresponds with periods of Oligocene upwelling, which was likely a main driver of early mobulid evolution. Although upwelling is not the only source of high productivity in the ocean, it does concentrate resources in a relatively small geographic area, often providing densities of food particles high enough to meet the large energy demands of filter-feeding marine mega fauna (Croll et al., 2005).

This is evident today, as contemporary mobulid distributions largely overlap with areas of high upwelling-related productivity in tropical and subtropical oceans (Fig. 6) and seasonal migration patterns that reflect temporal increases in upwelling (Anderson et al., 2011; Croll et al., 2012; Graham et al., 2012). The upwelling hypothesis has also been proposed for the mysticeti whales, whose early evolution in Southern Oceans coincides with the initiation of the Antarctic Circumpolar Current, and associated high upwelling-related productivity in this region during the Oligocene (Fordyce, 1980).

Pastene et al. (2007) suggested that periodic decreases in upwelling intensity through global warming could have facilitated allopatric speciation among pelagic populations of filter feeders. Upwelling has not been a stable phenomenon, but has waxed and waned following changes in the world's climate throughout the ages. Periods of global cooling with associated high upwelling intensities were alternated by extended periods of global warming (Zachos et al., 2001) during which upwelling areas (Schmittner, 2005; Fedorov et al., 2013; Ravelo et al., 2004) and related productivity (Diester-Haass et al., 2002; Marlow et al., 2000; Piela et al., 2012; Suto et al., 2012) were reduced. Hence, hypothetically, global warming may have resulted in fragmentation of the habitat of filter feeders, leading to different subpopulations eventually residing in smaller isolated regions, which may have facilitated speciation as suggested for the common minke whale (*Balaenoptera acutorostrata*) and Antarctic minke whale (*B. bonaerensis*) (Pastene et al., 2007). Our divergence estimates coincide broadly with several periods of global warming making such a mechanism conceivable for mobulids. Indeed, the divergence between Clades I and II (node 4, Fig. 4), and of *M. tarapacana*, *M. birostris* and *M. japanica* (nodes 5 and 6, Fig. 4), roughly coincide with the Miocene Climatic Optimum and the warm period leading up to it (~22–15 Mya) (Zachos et al., 2001). Similarly, estimated divergence of *M. thurstoni* (node 10, Fig. 4) coincides with another period of extended global warming during the Early Pliocene, which lasted from ~6 to 3.5 Mya (Fedorov et al., 2013).

The most recent speciation events between *M. eregoodootenkee* and *M. kuhlii*; *M. hypostoma* and *M. rochebrunei*; and *M. birostris* and *M. alfredi* occurred during the Glacial – Interglacial cycles of the Pleistocene (Kashiwagi et al., 2012; and the present study). Again, there was considerable variation in upwelling intensity and productivity during this period (Pedersen, 1983; Shaari et al., 2013). In addition, a major decrease in sea level during Pleistocene glacial periods may have further reinforced the isolation of populations by causing additional barriers to dispersal through the restriction of shallow seaways, especially in the Indo-West Pacific Ocean Coral Triangle (Pillans et al., 1998).

Molecular phylogenies based only on extant taxa often show an increase in speciation rates towards the present (Nee et al., 1994). This "pull of the present" results from the fact that lineages arising in the recent past are less likely to have become extinct, and therefore are over-represented in the phylogeny (Kubo and Iwasa, 1995; Nee et al., 1994). Although the use of a relaxed molecular clock, which accommodates rate variation over time, corrects for this

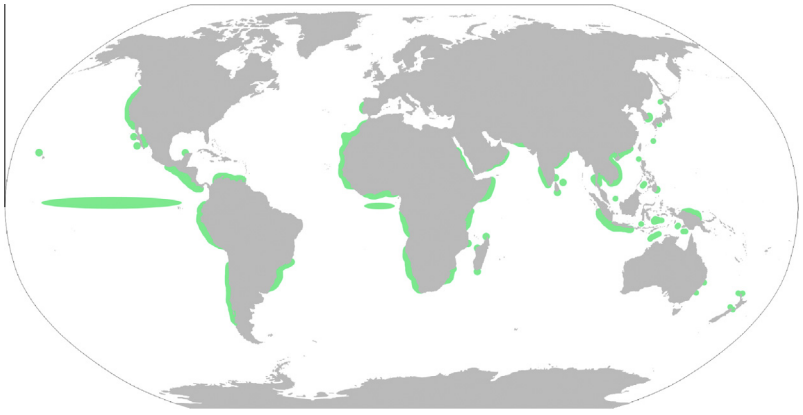

Fig. 6. Modern-day upwelling regions of the world, based on Alongi et al. (2012); Darbyshire (1967), Defant (1936), Fang et al. (2012), Furnestin (1959), Hasegawa et al. (2009), Ikema et al. (2013), Krishna (2011), Lafond (1954,1957), Lutjeharms and Machu (2000), Ma et al. (2013), Mazeika (1967), Rama Sastry and Myrland (1959), Roughan and Middleton (2002), Smith and Suthers (1999), Stommel and Wooster (1965), Swallow and Bruce (1966), Vinayachandran and Yamagata (1998), Warren et al. (1966), Wooster and Reid (1963), Wooster et al. (1967), Wyrtki (1961,1962, 1964, 1966) and Zaytsev et al. (2003).

issue to a certain degree (Morlon et al., 2011), we cannot exclude that the higher diversification rates during the Pleistocene are the consequence of this phenomenon.

The divergence between East Pacific *M. munkiana* and Atlantic species *M. rochebrunei* between 3.20 and 2.03 (node 13, Fig. 4) is consistent with the closing of the Isthmus of Panama, which most likely took place between 3.1 and 2.8 Mya (Coates et al., 2003; Coates and Obando, 1996). This event created a permanent separation between East Pacific and Atlantic mobulids as is the case for many marine species (Lessios, 2008) including various elasmobranchs (Daly-Engel et al., 2012; Keeney and Heist, 2006; Schultz et al., 2008; Stelbrink et al., 2010).

A genetic study of species boundaries between *M. birostris* and *M. alfredi* supported worldwide monophyly of nuclear RAG1 genotypes, but paraphyly of mitochondrial NADH5 genotypes around East Africa (Kashiwagi et al., 2012). The mitochondrial pattern was interpreted as possible secondary contact and introgression. Even if secondary contact occurred before speciation was complete, niche differentiation or possible behavioral incompatibilities could have been further promoted resulting in reproductive isolation. Kashiwagi et al. (2012) hypothesized that habitat specialization probably played an important role in the evolution of *M. birostris* and *M. alfredi*, since the two species generally exhibit habitat segregation between near-shore (*M. alfredi*) and offshore (*M. birostris*) environments (Marshall et al., 2009). Alternatively, due to the enormous migratory potential of (especially) *M. birostris*, it is conceivable that behavioral isolation and/or sexual selection for, e.g., size, played a more fundamental role in the divergence of the two species (Edelaar et al., 2008; Head et al., 2013; Weissing et al., 2011). Recently, a hybrid between *M. alfredi* and *M. birostris* was identified in the Red Sea, based on sequence analysis of the nuclear gene RAG1, which was heterozygous for two species-specific single nucleotide polymorphisms (Walter et al., 2014). This indicates that reproductive isolation between the two species may be less complete than previously reported.

4.4. Taxonomic issues

Our results regarding paraphyly of the genus *Mobula* are in agreement with previous studies based on molecular data (Naylor et al., 2012a; Aschliman et al., 2012a,b). Our results based on mitogenome data are also strongly congruent with data based on tooth morphology, which largely subdivides mobulids into the same clades as our mitogenome data set, with only *M. tarapacana* showing deviating tooth morphology from the rest of Clade I (Adnet et al., 2012; see Fig. S3).

To be descriptively useful, a genus should be monophyletic, with linear arrangements of species reflecting common ancestry (Wiley and Lieberman, 2011). Given that logic, *Manta* should be renamed to *Mobula*, since *Mobula* (Rafinesque-Schmaltz, 1810) has nomenclatural priority over *Manta* (Bancroft, 1829). Additionally, since *M. mobular* is the type species for the current genus *Mobula*, appropriate genus names for Clades II and III should be reviewed and possibly re-designated. However, Batoid classification is currently in transition, and a change at this stage provides no benefit for the spirit of taxonomic stability. We therefore recommend that the current genus designation be retained, pending confirmation by studies based on other methods, including comparative anatomy of all mobulid species.

Our single sample of *M. mobular* falls in a group together with *M. japanica* from the Atlantic, Pacific and Indian Oceans, based on both mitogenomic and nuclear data (Figs. 2–4). Genetic divergence between the two putative species is very small (mitogenomic coding region = 0.078–0.237%, nuclear = 0%), and falls within the range of divergence among *M. japanica* (mitogenomic coding region = 0.061–0.237%, nuclear = 0%). Morphologically, the two species are also highly similar, with small differences pertaining only to maximum DW (*M. mobular* has a larger maximum DW) morphometrics (*M. mobular* reaches a larger DW relative to the rest of the body), and tooth morphology (Adnet et al., 2012; Notarbartolo di Sciara, 1987). Combined, genetic and morphological data challenge the notion that *M. mobular* and *M. japanica* are two separate species. However, additional and population-level sampling, combined with genetic analysis and morphological examination are necessary before any conclusions can be drawn about the species status of *M. japanica*.

4.5. Conservation implications

All mobulids—*Manta* and *Mobula* (devil rays) share similar and vulnerable life histories (Hoenig and Gruber, 1990; Stevens, 2000; Dulvy et al., 2014) making them equally susceptible to threats from bycatch and targeted fisheries. Recently, conservation concerns have been raised for mobulids, with population declines recorded for several species (Couturier et al., 2012; Dulvy et al., 2008). Eight out of 11 mobulids are now listed as Near Threatened or worse on the International Union of the Conservation of Nature (IUCN) Red List, with the remaining three species listed as Data Deficient (Table 1). Manta rays are protected in several countries, including Mexico, Ecuador, the Republic of Maldives and the Philippines. Additionally, *M. birostris* is listed on Appendix I and II of the Convention of Migratory Species (CMS), and is protected by EU regulations (no. 43/2014), and *M. birostris*, *M. alfredi* and the putative third *Manta* species have received protection under the Convention on International Trade in Endangered Species (CITES) Appendix II, which was motivated by the desire to avoid utilization by strong export markets for the use of these animals' gill plates in Asian medicines. International protective legislation remains inadequate for *Mobula*. They are currently not listed by CMS or CITES, and are only protected in the Mediterranean Sea (*M. mobular*), Ecuador, the Philippines and the Republic of Maldives. Clearly, both *Manta* and *Mobula* need strong national and international protective measures in place given their similarities and shared vulnerabilities.

Futhermore, many unknowns remain in projecting the potential effect of climate change on upwelling systems (Bakun, 1990). Based on the IPCC Special Report on Emission Scenario A2, equatorial upwelling systems are projected to decrease by almost 30% by 2100 (Polovina et al., 2011). Such a reduction will potentially have a tremendous impact on mobulids and other species that are strongly dependent on the high productivity associated with upwelling. Regional extinctions, as well as biogeographic shifts in population movements to areas with sufficient food availability are likely outcomes.

In conclusion, the closely shared evolutionary history of mobulids in combination with ongoing threats from fisheries and climate change effects on upwelling and food supply, will promote the case for protection of all species in this vulnerable family of pelagic elasmobranchs.

Acknowledgments

We would like to thank Stella Boele-Bos and Irina Smolina for help with lab work; Robert Olson and Ernesto Altamirano from the Inter American Tropical Tuna Commission (IATTC) for providing samples from the Eastern Pacific Ocean; Colombo Estupiñan-Montaño for providing samples from Ecuador; Giuseppe Notarbartolo di Sciara and Fabrizio Serena for providing a sample of *M. mobular*; GrupoTortugero, volunteers of Proyecto Caguama, and Pablo, Felipe and Juan Cuevas for providing help with fieldwork in Baja California, Mexico; Felix Spee, Annamarie Krieg, Sanne Schepers and Erik Janssen for providing help with fieldwork in

Indonesia; Muséum national d'Histoire naturelle, Ichthyology collection, for providing samples from their collection; the Smithsonian Natural Museum of Natural History for providing samples from their collections; Gregor M. Cailliet for providing help with obtaining samples; and Island Conservation for help with fieldwork. This research was funded by a stipend to MP from the University of Groningen, Top-Master-Evolutionary Biology Program (2008–2012). Lab consumables, student support and field work for the research were supported by: the Monterey Bay Aquarium, the Marine Benthic Ecology and Evolution Dept., CEES, University of Groningen; the Ecology and Evolutionary Biology Dept., UC Santa Cruz; and the Marine Ecology Unit, Universitet i Nordland. All samples collected by D. Croll were collected under UC Santa Cruz IACUC permit CROLD00904.

Appendix A. Supplementary material

Supplementary data associated with this article can be found, in the online version, at http://dx.doi.org/10.1016/j.ympev.2014.10.012.

References

Adnet, S., Cappetta, H., Guinot, G., Notarbartolo di Sciara, G., 2012. Evolutionary history of the devilrays (Chondrichthyes: Myliobatiformes) from fossil and morphological inference. Zool. J. Linnean Soc. 166, 132–159.
Alongi, D.M., Wirasantosa, S., Wagey, T., Trott, L.A., 2012. Early diagenetic processes in relation to river discharge and coastal upwelling in the Aru Sea, Indonesia. Mar. Chem. 140–141, 10–23.
Anderson, R.C., Adam, M.S., Goes, J.I., 2011. From monsoons to mantas: seasonal distribution of *Manta alfredi* in the Maldives. Fish. Oceanogr. 20, 104–113.
Aschliman, N.C., 2014. Interrelationships of the durophagous stingrays (Batoidea: Myliobatidae). Environ. Biol. Fishes 97, 967–979.
Aschliman, N.C., Nishida, M., Miya, M., Inoue, J.G., Rosana, K.M., Naylor, G.J., 2012a. Body plan convergence in the evolution of skates and rays (Chondrichthyes: Batoidea). Mol. Phylogenet. Evol. 63, 28–42.
Aschliman, N.C., Claeson, K.M., McEachran, J.D., 2012b. Phylogeny of batoidea. In: Carrier, J.C., Musick, J.A., Heithaus, M.R. (Eds.), Biology of sharks and their relatives, second ed. CRC Press, Boca Raton, FL.
Avise, J.C., 1989. Gene trees and organismal histories: a phylogenetic approach to population biology. Evolution 43, 1192–1208.
Bakun, A., 1990. Global climate change and intensification of coastal ocean upwelling. Science 247, 198–201.
Bancroft, E.N., 1829. On the fish known in Jamaica as the sea-devil. Zool. J. Lond. 4 (16), 444–457 (art. 55).
Bancroft, E.N., 1831. On several fishes of Jamaica. Proc. Zool. Soc. Lond. 1, 134.
Benz, G.W., Deets, G.B., 1988. Fifty-one years later: an update on Entepherus, with a phylogenetic analysis of *Cecropidae Dana*, 1849 (Copepoda: Siphonostomatoida). Can. J. Zool. 66, 856–865.
Bigelow, H.B., Schroeder, W.C., 1953. Sawfishes, guitarfishes, skates, and rays. In: Bigelow, H.B., Schroeder, W.C. (Eds.), Fishes of the Western North Atlantic. Sears Foundation for Marine Research, Yale University, New Haven, CT.
Blakey, R.C., 2008. Gondwana paleogeography from assembly to breakup – a 500 m.y. odyssey. Geol. Soc. Am. Spec. 441.
Bleeker, P., 1859. Enumeratio specierum piscium hucusque in Archipelago Indico observatarum. Acta Societatis Scientiarum Indiarum Neerlandensium 3, 1–6.
Boersma, A., Silva, I.P., 1991. Distribution of Paleogene planktonic foraminifera – analogies with the recent? Palaeogeogr. Palaeoclim. Palaeoecol. 83, 29–48.
Bonnaterre, J.P., 1788. Tableau encyclopédique et méthodique des trois regnes de la nature, Panckoncke, Paris.
Bourdon, J., 1999. A fossil manta from the Early Pliocene (Zanclean) of North America. Tertiary Res. 19, 79–84.
Britten, R.J., 1986. Rates of DNA sequence evolution differ between taxonomic groups. Science 231, 1393–1398.
Brown, W.M., Prager, E.M., Wang, A., Wilson, A.C., 1982. Mitochondrial DNA sequences of primates: tempo and mode of evolution. J. Mol. Evol. 18, 225–239.
Cappetta, H., 1975. Contribution à l'étude des Sélaciens du groupe Monmouth (Campanien-Maestrichtien) du New Jersey. Palaeontogr. Abteilung A, 1–46.
Cappetta, H., 1985. Sur une nouvelle espèce de Burnhamia (Batomorphii, Mobulidae) dans l'Yprésien des Ouled Abdoun, Maroc. Tertiary Res. 7, 27–33.
Cappetta, H., 1987. Chondrichthyes: Mesozoic and Cenozoic Elasmobranchii. Gustav Fischer Verlag, Stuttgart.
Cappetta, H., 2006. Elasmobranchii post-Triadici (index generum et specierum). Backhuys Publishers, Leiden.
Cappetta, H., Stringer, G.L., 1970. A new batoid genus (Neoselachii: Myliobatiformes) from the Yazoo Clay (Upper Eocene) of Louisiana, U.S.A. Tertiary Res. 21, 51–56.
Case, G.R., 1980. A selachian fauna from the Trent Formation, lower Miocene (Aquitanian) of Eastern North Carolina. Palaeontogr. Abteilung A 171, 75–103.
Cerutti-Pereyra, F., Meekan, M.G., Wei, N.W., O'Shea, O., Bradshaw, C.J., Austin, C.M., 2012. Identification of rays through DNA barcoding: an application for ecologists. PLoS ONE 7 (6), E36479.
Charlesworth, J., Eyre-Walker, A., 2007. The other side of the nearly neutral theory, evidence of slightly advantageous back-mutations. Proc. Natl. Acad. Sci. USA 104, 16992–16997.
Cicimurri, D.J., Knight, J.L., 2009. Late Oligocene sharks and rays from the Chandler Bridge Formation, Dorchester County, South Carolina. Acta Palaeontol. Pol. 54, 627–647.
Claeson, K.M., O'Leary, M.A., Roberts, E.M., Sissoko, F., Bouaré, M., Tapanila, L., Goodwin, D., Gottfried, M.D., 2010. First Mesozoic record of the stingray *Myliobatis wurnoensis* from Mali and a phylogenetic analysis of Myliobatidae incorporating dental characters. Acta Palaeontol. Pol. 55, 655–674.
Coates, A.G., Obando, J.A., 1996. The geological evolution of the Central American Isthmus. Chicago Press, Chicago, IL.
Coates, A.G., Aubry, M.P., Berggren, W.A., Collins, L.S., Kunk, M., 2003. Early Neogene history of the Central American arc from Bocas del Toro, western Panama. Geol. Soc. Am. Bull. 115, 271–287.
Coles, R.J., 1916. Natural history notes on the devil-fish, *Manta birostris* (Walbaum) and *Mobula olfersi* (Müller). Bull. Am. Museum Nat. History XXXV, 649–657.
Compagno, L.J.V., Last, P.R., 1999. Mobulidae. The Living Marine Resources of the Western Central Pacific. FAO, Rome.
Cortés, E., Papastamatiou, Y.P., Carlson, J.K., Ferry-Graham, L., Wetherbee, B.M., Cyrino, J.E.P., Bureau, D.P., Kapoor, B.G., 2008. An overview of the feeding ecology and physiology of elasmobranch fishes. In: Cyrino, J.E.P., Bureau, D., Kapoor, B.G. (Eds.), Feeding and Digestive Functions of Fishes. Science Publishers, Edenbridge.
Couturier, L.I., Marshall, A.D., Jaine, F.R., Kashiwagi, T., Pierce, S.J., Townsend, K.A., Weeks, S.J., Bennett, M.B., Richardson, A.J., 2012. Biology, ecology and conservation of the Mobulidae. J. Fish Biol. 80, 1075–1119.
Crisp, M.D., Cook, L.G., 2009. Explosive radiation or cryptic mass extinction? Interpreting signatures in molecular phylogenies. Evolution 63, 2257–2265.
Croll, D.A., Marinovic, B., Benson, S., Chavez, F.P., Black, N., Ternuilo, R., Tershy, B., 2005. From wind to whales: trophic links in a coastal upwelling system. Mar. Ecol. Prog. Ser. 289, 117–130.
Croll, D.A., Newton, K.M., Weng, K., Galván-Magaña, F., O'Sullivan, J., Dewar, H., 2012. Movement and habitat use by the spine-tail devil ray in the Eastern Pacific Ocean. Mar. Ecol. Prog. Ser. 465, 193–200.
Cuevas-Zimbrón, E., Sosa-Nishizaki, O., Pérez-Jiménez, J.C., O'Sullivan, J.B., 2012. An analysis of the feasibility of using caudal vertebrae for ageing the spinetail devilray, *Mobula japanica* (Müller and Henle, 1841). Environ. Biol. Fishes 96, 907–914.
Cummings, M.P., Otto, S., Wakely, J., 1995. Sampling properties of DNA sequence data in phylogenetic analysis. Mol. Biol. Evol. 12, 814–822.
Daly-Engel, T.S., Seraphin, K.D., Holland, K.N., Coffey, J.P., Nance, H.A., Toonen, R.J., Bowen, B.W., 2012. Global phylogeography with mixed-marker analysis reveals male-mediated dispersal in the endangered scalloped hammerhead shark (*Sphyrna lewini*). PLoS ONE 7, e29986.
Darbyshire, M., 1967. The surface waters off the coast of Kerala, southwest India. Deep-Sea Res. 14, 295–320.
De Carvalho, M.R., Maisey, J.G., Grande, L., 2004. Freshwater stingrays of the Green River formation of Wyoming (early Eocene), with the description of a new genus and species and an analysis of its phylogenetic relationships (Chondrichthyes: Myliobatiformes). Bull. AMNH 284, 1–36.
Defant, A., 1936. Das Kaltwasserauftriebsgebiet vor des Küste Sudwestafrikas. Landesk. Forsch. 1936, 52–66.
Diester-Haass, L., Meyers, P.A., Laurence, V., 2002. The late Miocene onset of high productivity in the Benguela Current upwelling system as part of a global pattern. Mar. Geol. 180, 87–103.
Dixon, M.T., Hillis, D.M., 1993. Ribosomal RNA secondary structure: compensatory mutations and implications for phylogenetic analysis. Mol. Biol. Evol. 10, 256–267.
Drummond, A.J., Rambaut, A., 2007. BEAST: Bayesian evolutionary analysis by sampling trees. BMC Evol. Biol. 7, 214.
Drummond, A.J., Suchard, M.A., 2010. Bayesian random local clocks, or one rate to rule them all. BMC Biol. 8, 114.
Drummond, A.J., Nicholls, G.K., Rodrigo, A.G., Solomon, W., 2002. Estimating mutation parameters, population history and genealogy simultaneously from temporally spaced sequence data. Genetics 161 (3), 1307–1320.
Drummond, A.J., Suchard, M.A., Xie, D., Rambaut, A., 2012. Bayesian phylogenetics with BEAUti and the BEAST 1.7. Mol. Biol. Evol. 29 (8), 1969–1973.
Dudgeon, C.L., Blower, D.C., Broderick, D., Giles, J.L., Holmes, B.J., Kashiwagi, T., Kruck, N.C., Morgan, J.A., Tillett, B.J., Ovenden, J.R., 2012. A review of the application of molecular genetics for fisheries management and conservation of sharks and rays. J. Fish Biol. 80, 1789–1843.
Dulvy, N.K., Baum, J.K., Clarke, S., Compagno, L.J.V., Cortés, E., Domingo, A., Fordham, S., Fowler, S., Francis, M.P., Gibson, C., Martínez, J., Musick, J.A., Soldo, A., Stevens, J.D., Valenti, S., 2008. You can swim but you can't hide: the global status and conservation of oceanic pelagic sharks and rays. Aquat. Conserv.: Mar. Freshw. Ecosyst. 18, 459–482.
Dulvy, N.K., Pardo, S.A., Simpfendorfer, C.A., Carlson, J.K., 2014. Diagnosing the dangerous demography of manta rays using life history theory. PeerJ 2, e400.
Dunn, K.A., McEachran, J.D., Honeycutt, R.L., 2003. Molecular phylogenetics of myliobatiform fishes (Chondrichthyes: Myliobatiformes), with comments on the effects of missing data on parsimony and likelihood. Mol. Phylogenet. Evol. 27, 259–270.

Edelaar, P., Siepielski, A.M., Clobert, J., 2008. Matching habitat choice causes directed gene flow: a neglected dimension in evolution and ecology. Evolution 62, 2462–2472.
Fang, G., Wang, G., Fang, Y., Fang, W., 2012. A review on the South China Sea western boundary current. Acta Oceanol. Sin. 31, 1–10.
Fedorov, A.V., Brierley, C.M., Lawrence, K.T., Liu, Z., Dekens, P.S., Ravelo, A.C., 2013. Patterns and mechanisms of early Pliocene warmth. Nature 496, 43–49.
Fordyce, R.E., 1980. Whale evolution and Oligocene Southern Ocean environments. Palaeogeogr. palaeoclim. palaeoecol. 31, 319–336.
Furnestin, J., 1959. Hydrologie du Maroc Atlantique. Revue. Trav. Inst. (scient tech) Pêch. Marit. 23, 5–77.
Gadig, O., Neto, D., 2014. Notes on the feeding behaviour and swimming pattern of *Manta alfredi* (Chondrichthyes, Mobulidae) in the Red Sea. Acta Ethologica 17, 119–122.
Galtier, N., Nabholz, B., Glemin, S., Hurst, G.D., 2009. Mitochondrial DNA as a marker of molecular diversity: a reappraisal. Mol. Ecol. 18, 4541–4550.
Garcia, V.B., Lucifora, L.O., Myers, R.A., 2008. The importance of habitat and life history to extinction risk in sharks, skates, rays and chimaeras. Proc. Biol. Sci. 275, 83–89.
Gonzalez-Isais, M., Dominguez, H.M., 2004. Comparative anatomy of the superfamily Myliobatoidea (Chondrichthyes) with some comments on phylogeny. J. Morphol. 262, 517–535.
Graham, R.T., Witt, M.J., Castellanos, D.W., Remolina, F., Maxwell, S., Godley, B.J., Hawkes, L.A., 2012. Satellite tracking of manta rays highlights challenges to their conservation. PLoS ONE 7, e36834.
Haddrill, P.R., Halligan, D.L., Tomaras, D., Charlesworth, B., 2007. Reduced efficacy of selection in regions of the *Drosophila* genome that lack crossing over. Genome Biol. 8 (2), R18.
Han, M.V., Zmasek, C.M., 2009. PhyloXML: XML for evolutionary biology and comparative genomics. BMC Bioinformatics 10, 356.
Hasegawa, T., Ando, K., Mizundo, K., Lukas, R., 2009. Coastal upwelling along the North Coast of Papua New Guinea and SST cooling over the pacific warm pool: a case study for the 2002/03 El Niño Event. J. Oceanogr. 65, 817–833.
Head, M.L., Kozak, G.M., Boughman, J.W., 2013. Female mate preferences for male body size and shape promote sexual isolation in threespine sticklebacks. Ecol. Evol. 3, 2183–2196.
Herman, J., Hovestadt-Euler, M., Hovestadt, D.C., Stehmann, M., 2000. Contributions to the study of the comparative morphology of teeth and other relevant ichthyodorulites in living supra-specific taxa of Chondrichthyan fishes. Part B: Batomorphii 4c: Order: Rajiformes – Suborder Myliobatoidei – Superfamily Dasyatoidea – Family Dasyatidae – Subfamily Dasyatinae – Genus: *Urobatis*, Subfamily Potamotrygoninae – Genus: *Potamotrygon*, Superfamily Plesiobatoidea – Family Plesiobatidae – Genus: *Plesiobatis*, Superfamily Myliobatoidea – Family Myliobatidae – Subfamily Myliobatinae – Genera: *Aetobatus*, *Aetomylaeus*, *Myliobatis* and *Pteromylaeus*, Subfamily Rhinopterinae – Genus: *Rhinoptera* and Subfamily Mobulinae – Genera: *Manta* and *Mobula*. Addendum 1 to 4a: erratum to Genus *Pteroplatytrygon*. Bull. Inst. R. Sci. Nat. Belg. Biol. 70, 5–67.
Hoarau, G., Coyer, J.A., Stam, W.T., Olsen, J.L., 2006. A fast and inexpensive DNA extraction/purification protocol for brown macroalgae. Mol. Ecol. Notes 7, 191–193.
Hoelzel, A.R., Natoli, A., Dahlheim, M.E., Olavarria, C., Baird, R.W., Black, N.A., 2002. Low worldwide genetic diversity in the killer whale (Orcinus orca): implications for demographic history. Proc. Biol. Sci. 269, 1467–1473.
Hoenig, J.M., Gruber, S.H., 1990. Life-History Patterns in the Elasmobranchs: Implications for Fisheries Management. NOAA Technical Report.
Huelsenbeck, J., Ronquist, F., 2001. MRBAYES: Bayesian inference of phylogenetic trees. Bioinformatics 17, 754–755.
Ikema, T., Bryant, R.G., Bigg, G.R., 2013. Environmental controls at multiple scales for the western Pacific: an Okinawan case study. Estuar. Coast Shelf Sci. 128, 52–63.
Kashiwagi, T., Marshall, A.D., Bennett, M.B., Ovenden, J.R., 2012. The genetic signature of recent speciation in manta rays (*Manta alfredi* and *M. birostris*). Mol. Phylogenet. Evol. 64, 212–218.
Keeney, D.B., Heist, E.J., 2006. Worldwide phylogeography of the blacktip shark (*Carcharhinus limbatus*) inferred from mitochondrial DNA reveals isolation of western Atlantic populations coupled with recent Pacific dispersal. Mol. Ecol. 15, 3669–3679.
Kelchner, S.A., Thomas, M.A., 2007. Model use in phylogenetics: nine key questions. Trends Ecol. Evol. 22, 87–94.
Kollias, S., Poortvliet, M., Smolina, I., Hoarau, G., submitted for publication. A Quick and Easy Method of Mitochondrial Genome Capture for NGS Applications.
Krefft, J.L.G., 1868. *Deratoptera alfredi* (Prince Alfred's ray). Illustr. Sydney News 5 (3), 9.
Krishna, K.M., 2011. Satellite surveillance of upwelling along the east coast of India. Mar. Geod. 34, 181–187.
Kubo, T., Iwasa, Y., 1995. Inferring the rates of branching and extinction from molecular phylogenies. Evolution 49, 694–704.
Lafond, E.C., 1954. On upwelling and sinking off the east coast of India. Andhra Univ. Mem. Oceanogr. 1.
Lafond, E.C., 1957. Oceanographic studies in the Bay of Bengal. Proc. Indian Acad. Sci. (B) 46, 1–46.
Lanfear, R., Calcott, B., Ho, S.Y., Guindon, S., 2012. Partitionfinder: combined selection of partitioning schemes and substitution models for phylogenetic analyses. Mol. Biol. Evol. 29, 1695–1701.
Last, P.R., Stevens, J.D., 2009. Sharks and Rays of Australia. CSIRO Marine and Atmospheric Research. CSIRO Publishing, Australia.
Laurito Mora, C.A., 1999. Los selaceos fosiles de la localidad de Alto Guayacan (y otros ictiolitos associados): Mioceno Superior-Plioceno Inferior de Limòn, Costa Rica, Guila Imprenta, San José.
Lessios, H.A., 2008. The great American schism: divergence of marine organisms after the rise of the Central American Isthmus. Annu. Rev. Ecol. Evol. Syst. 39, 63–91.
Lloyd, R.E., 1908. On two species of eagle-rays with notes on the skull of the genus *Ceratoptera*. Rec. Indian Museum (Calcutta) 2, 175–180.
Lovejoy, N.R., 1996. Systematics of myliobatoid elasmobranchs: with emphasis on the phylogeny and historical biogeography of neotropical freshwater stingrays (Potamotrygonidae: Rajiformes). Zool. J. Linnean Soc. 117, 207–257.
Lutjeharms, J.R.E., Machu, E., 2000. An upwelling cell inshore of the East Madagascar current. Deep Sea Res. Part I: Oceanogr. Res. Pap., 2405–2411.
Ma, W., Chai, F., Xiu, P., Xue, H., Tian, J., 2013. Modeling the long-term variability of phytoplankton functional groups and primary productivity in the South China Sea. J. Oceanogr. 69, 527–544.
Marlow, J.R., Lange, C.B., Wefer, G., Rosell-Mele, A., 2000. Upwelling intensification as part of the Pliocene-Pleistocene climate transition. Science 290, 2288–2291.
Marshall, A.D., Bennett, M.B., 2010. Reproductive ecology of the reef manta ray *Manta alfredi* in southern Mozambique. J. Fish Biol. 77, 169–190.
Marshall, A.D., Compagno, L.J.V., Leonard, J.V., Bennett, M.B., 2009. Redescription of the genus *Manta* with resurrection of *Manta alfredi* (Krefft, 1868) (Chondrichthyes; Myliobatoidei; Mobulidae). Zootaxa 2301, 1–28.
Martin, A.P., 1995. Mitochondrial DNA sequence evolution in sharks: rates, patterns and phylogenetic inference. Mol. Biol. Evol. 12, 1114–1123.
Martin, A.P., 1999. Substitution rates of organelle and nuclear genes in sharks: implicating metabolic rate (again). Mol. Biol. Evol. 16, 996–1002.
Martin, A.P., Palumbi, S.R., 1993. Body size, metabolic rate, generation time, and the molecular clock. Proc. Natl. Acad. Sci. USA 90, 4087–4091.
Martin, A.P., Naylor, G.J., Palumbi, S.R., 1992. Rates of mitochondrial DNA evolution in sharks are slow compared with mammals. Nature 357, 153–155.
Mazeika, P.A., 1967. Thermal domes in the Eastern Tropical Atlantic. Limnol. Oceanogr. 12, 537–539.
McEachran, J.D., Aschliman, N.C., 2004. Phylogeny of Batoidea. In: Carrier, J.C., Musick, J.A., Heithaus, M.R. (Eds.), Biology of Sharks and Their Relatives. CRC Press, Boca Raton, FL.
McEachran, J.D., Dunn, K.A., Miyake, T., 1996. Interrelationships of the batoid fishes (Chondrichthyes, Batoidea). In: Stiassny, M.L.J., Parenti, L.R., Johnson, G.D. (Eds.), Interrelationships of Fishes. Academic Press, San Diego, CA.
Moore, W.S., 1995. Inferring phylogenies from mtDNA variation: mitochondrial-gene trees versus nuclear-gene trees. Evolution 49, 718–726.
Morin, P.A., Archer, F.I., Foote, A.D., Vilstrup, J., Allen, E.E., Wade, P., Durban, J., Parsons, K., Pitman, R., Li, L., Bouffard, P., Abel Nielsen, S.C., Rasmussen, M., Willerslev, E., Gilbert, M.T., Harkins, T., 2010. Complete mitochondrial genome phylogeographic analysis of killer whales (Orcinus orca) indicates multiple species. Genome Res. 20, 908–916.
Moritz, C., 1994. Applications of mitochondrial DNA analysis in conservation: a critical review. Mol. Ecol. 3, 401–411.
Morlon, H., Parsons, T.L., Plotkin, J.B., 2011. Reconciling molecular phylogenies with the fossil record. Proc. Natl. Acad. Sci. USA 108, 16327–16332.
Müller, K., 2005. SeqState – primer design and sequence statistics for phylogenetic DNA data sets. Appl. Bioinformatics 4, 65–69.
Müller, J., Henle, J., 1841. Systematische beschreibung der plagiostomen. Verlag von Veit & Co., Berlin.
Nabholz, B., Glemin, S., Galtier, N., 2008. Strong variations of mitochondrial mutation rate across mammals-the longevity hypothesis. Mol. Biol. Evol. 25, 120–130.
Naylor, G.J.P., Caira, J.N., Jensen, K., Rosana, K.A.M., Straube, N., Lakner, C., 2012a. Elasmobranch phylogeny: a mitochondrial estimate based on 595 species. In: Carrier, J.C., Musick, J.A., Heithaus, M.R. (Eds.), Biology of Sharks and Their Relatives. CRC Press, Boca Raton, FL.
Naylor, G.J.P., Caira, J.N., Jensen, K., Rosana, K.A.M., White, W.T., Last, P.R., 2012b. A DNA sequence-based approach to the identification of shark and ray species and its implications for global elasmobranch diversity and parasitology. Bull. Am. Mus. Nat. Hist. 367, 1–262.
Nee, S., May, R.M., Harvey, P.H., 1994. The reconstructed evolutionary process. Philos. Trans. Roy. Soc. Lond. B 344, 305–311.
Nishida, K., 1990. Phylogeny of the Suborder Myliobatidoidei. Hokkaido University.
Notarbartolo di Sciara, G., 1987. A revisionary study of the genus *Mobula* Rafinesque, 1810 (Chondrichthyes: Mobulidae) with the description of a new species. Zool. J. Linnean Soc. 91, 1–91.
Nylander, J.A., Wilgenbusch, J.C., Warren, D.L., Swofford, D.L., 2008. AWTY (are we there yet?): a system for graphical exploration of MCMC convergence in Bayesian phylogenetic inference. Bioinformatics 24, 581–583.
Olson, P.D., Caira, J.N., Jensen, K., Overstreet, R.M., Palm, H.W., Beveridge, I., 2010. Evolution of the trypanorhynch tapeworms: parasite phylogeny supports independent lineages of sharks and rays. Int. J. Parasitol. 40, 223–242.
Paig-Tran, E.W., Kleinteich, T., Summers, A.P., 2013. The filter pads and filtration mechanisms of the devil rays: variation at macro and microscopic scales. J. Morphol. 274, 1026–1043.
Pastene, L.A., Goto, M., Kanda, N., Zerbini, A.N., Kerem, D., Watanabe, K., Bessho, Y., Hasegawa, M., Nielsen, R., Larsen, F., Palsboll, P.J., 2007. Radiation and speciation of pelagic organisms during periods of global warming: the case of

the common minke whale, *Balaenoptera acutorostrata*. Mol. Ecol. 16, 1481–1495.
Pedersen, T.F., 1983. Increased productivity in the Eastern Equatorial Pacific during the last glacial maximum (19,000 to 14,000 yr B.P). Geology 11, 16–19.
Pellegrin, J., 1901. Sur une raie cornue gigantesque pechee à Oran. Bull. Muséum Natl. d'Historire Naturelle 7, 327–328.
Pfeil, F.H., 1981. Eine nektonische Fischfauna aus dem unteroligozänen Schönecker Fischschiefer des Galon-Grabens in Oberbayern. Geol. Bavarica 82, 357–388.
Philippi, R.A., 1892. Algunos peces de Chile. Las rayas. Callorrhynchus i Orthagoriscus Chilenos. Anales del Museo Nacional de Chile. Primera seccion. Zoología No. 3: 1 + 1-16 + 1, Pls. 1-6.
Picot, L., Becker, D., Cavin, L., Pirkenseer, C., Lapaire, F., Rauber, G., Hochuli, P.A., Berger, J.-P., 2008. Sédimentologie et paléontologie des paléoenvironnements côtiers Rupéliens de la Molasse marine rhénane dans le Jura suisse. Swiss J. Geosci. 101, 483–513.
Piela, C., Lyle, M., Marcantonio, F., Baldauf, J., Olivarez Lyle, A., 2012. Biogenic sedimentation in the equatorial Pacific: carbon cycling and paleoproduction, 12–24 Ma. Paleoceanography 27, PA2204. http://dx.doi.org/10.1029/2011PA002236.
Pillans, B., Chappell, J., Naish, T.R., 1998. A review of the Milankovitch climatic beat: template for Plio-Pleistocene sea-level changes and sequence stratigraphy. Sediment. Geol. 122, 5–21.
Polovina, J.J., Dunne, J.P., Woodworth, P.A., Howell, E.A., 2011. Projected expansion of the subtropical biome and contraction of the temperate and equatorial upwelling biomes in the North Pacific under global warming. ICES J. Mar. Sci. 68, 986–995.
Poortvliet, M., Hoarau, G., 2013. The complete mitochondrial genome of the spinetail devilray, *Mobula japanica*. MDN 24, 28–30.
Posada, D., 2008. jModelTest: phylogenetic model averaging. Mol. Biol. Evol. 25, 1253–1256.
Presgraves, D.C., 2005. Recombination enhances protein adaptation in Drosophila melanogaster. Curr. Biol. 15, 1651–1656.
Purdy, R.W., Schneider, V.P., Applegate, S.P., McLellan, J.H., Meyer, R.L., Slaughter, B.H., 2001. The Neogene sharks, rays, and bony fishes from Lee Creek Mine, Aurora, North Carolina. In: Clayton, E.R., Bohaska, D.J. (Eds.), Geology and Paleontology of the Lee Creek Mine, North Carolina, III. Smithsonian Institution Press, Washington, DC.
Rafinesque-Schmaltz, C.S., 1810. Indice d'ittiologia siciliana ossia catalogo metodico dei nomi latini, italiani e siciliani dei pesci, che si rinvengono in Sicilia. Messina.
Rama Sastry, A.A., Myrland, P., 1959. Distribution of temperature, salinity and density in the Arabian Sea along the south Malabar coast (South India) during the post-monsoon season. Indian J. Fish. 6, 223–255.
Rambaut, A., Drummond, A.J., 2009. Tracer v1.5. <http://tree.bio.ed.ac.uk/software/tracer/>.
Ravelo, A.C., Andreasen, D.H., Lyle, M., Lyle, A.O., Wara, M.W., 2004. Regional climate shifts caused by gradual global cooling in the Pliocene epoch. Nature 429, 263–267.
Revell, L.J., Harmon, L.J., Glor, R.E., 2005. Underparameterized model of sequence evolution leads to bias in the estimation of diversification rates from molecular phylogenies. Syst. Biol. 54, 973–983.
Roughan, M., Middleton, J.H., 2002. A comparison of observed upwelling mechanisms off the east coast of Australia. Cont. Shelf Res. 22, 2551–2572.
Schmittner, A., 2005. Decline of the marine ecosystem caused by a reduction in the Atlantic overturning circulations. Nature 434, 628–633.
Schultz, J.K., Feldheim, K.A., Gruber, S.H., Ashley, M.V., McGovern, T.M., Bowen, B.W., 2008. Global phylogeography and seascape genetics of the lemon sharks (genus *Negaprion*). Mol. Ecol. 17, 5336–5348.
Shaari, H.B., Yamamoto, M., Irino, T., 2013. Enhanced upwelling in the Eastern Equatorial Pacific at the last five glacial terminations. Palaeogeogr. Palaeoclim. Palaeoecol. 386, 8–15.
Shirai, S., 1996. Phylogenetic interrelationships of neoselachians (Chondrichthyes: Euselachii). In: Stiassny, M.L.J., Parenti, L.R., Johnson, G.D. (Eds.), Interrelationships of Fishes. Academic Press, San Diego, CA.
Simmons, M.P., Ochoterena, H., 2000. Gaps as characters in sequence-based phylogenetic analyses. Syst. Biol. 49, 369–381.
Smith, K.A., Suthers, I.M., 1999. Displacement of diverse ichthyoplankton assemblages by a coastal upwelling event on the Sydney shelf. Mar. Ecol. Prog. Ser. 176, 49–62.
Stamatakis, A., 2006. RAxML-VI-HPC: maximum likelihood-based phylogenetic analyses with thousands of taxa and mixed models. Bioinformatics 22, 2688–2690.
Stelbrink, B., Von Rintelen, T., Cliff, G., Kriwet, J., 2010. Molecular systematics and global phylogeography of angel sharks (genus Squatina). Mol. Phylogenet. Evol. 54, 395–404.
Stevens, J., 2000. The effects of fishing on sharks, rays, and chimaeras (chondrichthyans), and the implications for marine ecosystems. ICES J. Mar. Sci. 57, 476–494.
Stommel, H., Wooster, W.S., 1965. Reconnaissance of the Somali Current during the southwest monsoon. Proc. Natl. Acad. Sci. USA 54, 8–13.
Sullivan, J., Swofford, D.L., Naylor, G.J.P., 1999. The effect of taxon sampling on estimating rate heterogeneity parameters of maximum-likelihood models. Mol. Biol. Evol. 16 (10), 1347–1356.
Suto, I., Kawamura, K., Hagimoto, S., Teraishi, A., Tanaka, Y., 2012. Changes in upwelling mechanisms drove the evolution of marine organisms. Palaeogeogr. Palaeoclim. Palaeoecol. 339–341, 39–51.
Swallow, J.C., Bruce, J.G., 1966. Current measurements off the Somali coast during the southwest monsoon of 1964. Deep-Sea Res. 13, 861–888.
Tamura, K., Peterson, D., Peterson, N., Stecher, G., Nei, M., Kumar, S., 2011. MEGA5: molecular evolutionary genetics analysis using maximum likelihood, evolutionary distance, and maximum parsimony methods. Mol. Biol. Evol. 28, 2731–2739.
Vaillant, L.L., 1879. Note sur une nouvelle espèce d'élasmobranche hypotrème, le *Cephaloptera rochebrunei*. Bull. Soc. Philomatique, Paris 7, 187–188.
Vilstrup, J.T., Ho, S.Y., Foote, A.D., Morin, P.A., Kreb, D., Krutzen, M., Parra, G.J., Robertson, K.M., De Stephanis, R., Verborgh, P., Willerslev, E., Orlando, L., Gilbert, M.T., 2011. Mitogenomic phylogenetic analyses of the Delphinidae with an emphasis on the Globicephalinae. BMC Evol. Biol. 11, 65.
Vinayachandran, P.N., Yamagata, T., 1998. Monsoon response of the sea around Sri Lanka: generation of thermal domes and anticyclonic vortices. J. Phys. Oceanogr. 28 (10), 1946–1960.
Walbaum, J.J., 1792. Petri artedi sueci genera piscium. Grypeswaldiae, Röse.
Walter, R.P., Kessel, S.T., Alhasan, N., Fisk, A.T., Heath, D.D., Chekchak, T., Klaus, R., Younis, M., Hill, G., Jones, B., Braun, C.D., Berumen, M.L., DiBattista, J.D., Priest, M.A., Hussey, N.E., 2014. First record of living *Manta alfredi* × *Manta birostris* hybrid. Mar. Biodivers. 44, 1–2.
Warren, B., Stommel, H., Swallow, J.C., 1966. Water masses and patterns of flow in the Somali Basin during the southwest monsoon of 1964. Deep-Sea Res. 13, 825–860.
Weissing, F.J., Edelaar, P., Van Doorn, G.S., 2011. Adaptive speciation theory: a conceptual review. Behav. Ecol. Sociobiol. 65, 461–480.
Wielstra, B., Arntzen, J.W., 2011. Unraveling the rapid radiation of crested newts (*Triturus cristatus* superspecies) using complete mitogenomic sequences. BMC Evol. Biol. 11, 162.
Wiley, E.O., Lieberman, B.S., 2011. Phylogenetics: Theory and Practice of Phylogenetic Systematics, second ed. John Wiley & Sons Inc., Hoboken, NJ.
Woodward, A.S., 1889. Catalogue of the Fossil Fishes in the British Museum (Natural History), Part 1: Containing the Elasmobranchii. London, UK.
Woolfit, M., 2009. Effective population size and the rate and pattern of nucleotide substitutions. Biol. Lett. 5, 417–420.
Wooster, W.S., Reid, J.L., 1963. Eastern Boundary Currents. Wiley-Interscience, New York, NY.
Wooster, W.S., Schaefer, M.B., Robinson, M.K., 1967. Atlas of the Arabian Sea for Fishery Oceanography. La Jolla, University of California, Institute of Marine Resources.
Wu, C.I., Li, W.H., 1985. Evidence for higher rates of nucleotide substitution in rodents than in man. Proc. Natl. Acad. Sci. USA 82, 1741–1745.
Wyrtki, K., 1961. Physical oceanography of the Southeast Asian waters. Naga Rep. 2, 195.
Wyrtki, K., 1962. The upwelling in the region between Java and Australia during the southeast monsoon. Aust. J. Mar. Freshwat. Res. 13, 217–225.
Wyrtki, K., 1964. Upwelling in the Costa Rica Dome. Fishery Bull. Fish Wildl. Serv. US 63, 355–372.
Wyrtki, K., 1966. Oceanography of the Eastern equatorial Pacific Ocean. Oceanogr. Mar. Biol. Ann. Rev. 4, 33–68.
Yu, L., Li, Y.W., Ryder, O.A., Zhang, Y.P., 2007. Analysis of complete mitochondrial genome sequences increases phylogenetic resolution of bears (Ursidae), a mammalian family that experienced rapid speciation. BMC Evol. Biol. 7, 198.
Zachos, J.C., Quinn, T.M., Salamy, K.A., 1996. High-resolution ($10^{(4)}$ years) deep-sea foraminiferal stable isotope records of the Eocene-Oligocene climate transition. Paleoceanography 11, 251–266.
Zachos, J., Pagani, M., Sloan, L., Thomas, E., Billups, K., 2001. Trends, rhythms, and aberrations in global climate 65 Ma to present. Science 292, 686–693.
Zaytsev, O., Cervantes-Duarte, R., Montante, O., Gallegos-Garcia, A., 2003. Coastal upwelling activity on the Pacific shelf of the Baja California peninsula. J. Oceanogr. 59, 489–502.